University of Groningen

Kapteyn Astronomical Institute

Master Thesis

How to Find Galaxy-Scale Strong Gravitationally Lensed Quasar Candidates in the Kilo Degree Survey

Casper Blokzijl

Supervisors:
G. Verdoes-Kleijn & H. Buddelmeijer

3rd February, 2014

Abstract

The goal of this thesis is to develop a method for finding galaxy-scale strong gravitationally lensed quasar(QSO) candidates in the Kilo Degree Survey(KiDS). KiDS is a relatively new survey carried out with the OmegaCAM at Paranal, Chile. Observations are made in the optical regime (ugri filters), and KiDS has better image quality than some other surveys done in similar wavebands. KiDS officially released their first data (KiDS-ESO-DR1) recently.

We investigate the potential of KiDS for finding strong lenses using earlier work of Oguri and Marshall (Oguri and Marshall, 2010). We conclude that we can expect 200-450 strong gravitational lenses in KiDS. We take a look at known and mock lenses, to more reliantly understand what we can expect of strong lenses in KiDS. From the known lenses we learn that SExtractor does not detect the lens galaxy. Using detected QSO-like blue point sources is therefore the best way to find lenses using KiDS.

We test 2 different methods for finding strong lens candidates in KiDS: by using existing QSO/-Luminous Red Galaxy(LRG) catalogs and by using typical lens characteristics. We use the BOSS and LRGS catalog. By using these catalogs we find 4 interesting strong lens candidates, none of which we are convinced are real lenses. Completeness when using this method is relatively low, and most catalogs are probably filtered for lenses. For the second method we developed a decision tree, based on typical u-i values and separations of blue point sources consistent with strong lensed QSOs. We have time to test 3 parts of the decision tree, and not the full decision tree. The methods that we test are: blue point sources u-i<2, blue pairs u-i<2 and separation<10 arcsec, and blue pairs u-i<3 and separation<10 arcsec. With theses methods we find 3 strong lens candidates, but none of them are believed to be real lenses. Out of all described methods, blue pairs u-i<2 is theoretically the most potent one, with the highest completeness/contamination ratio.

Finally, we compare the expected number of lenses and the time it takes until you potentially have found them with KiDS to those of other surveys, using a multi-criteria analysis. KiDS ranks position 4 out of 5 surveys, which means KiDS does not have the highest potential to invest in the search for finding new lenses in the future.

I recommend that work should continue on implementing the initially developed decision tree, since the initially developed decision tree has not yet been tested. Based on those results it can be decided if this approach is going to work at all. Catalogs are not the way to go. Investigating how lensing galaxies can be detected with SExtractor, and if they can be used to find strong lenses might also be interesting. Other ways could be to develop LensTractor (lens fitting software made by Phil Marshall) into a working tool for finding lenses. Implementing candidates into SpaceWarps might be a useful application that can be implemented at the Infoversum.

CONTENTS

Prologue: The Science, Business and Policy Master Program

An astronomy student in the master phase at the University of Groningen (RUG) can choose between different master programs: the research master, the instrumentation master or the science, business and policy (SBP) master. Because I realized that my ambitions are not in astronomical research or instrumentation, I chose to do the SBP master (in the summer of 2012). Since the SBP master is not a common program for a master student astronomy, it's useful to describe how this program actually works.

The program is divided into two equal parts, an astronomical part and a SBP part, of both one year in length, adding up to a total of 120 EC (EC is short for ECTS. In Holland ECTS stand for European Credit Transfer System, 1 EC is 28 hours of work, 60EC is one full year of study). The astronomical part consists of 30EC courses and a 30EC master thesis. In contrast to the other master programs, this master program has a 30 EC thesis, instead of a 60EC. The SBP part consists of 20EC courses and a 40EC internship. See Table 1 for an overview of the structure of the study. Before starting the internship, the student is required to finish his/her master thesis first.

Table 1: Overview of the master program science, business and policy.

Part of program	EC
Astronomy	
Courses	30
Master Thesis	30
SBP	
Courses	20
Internship	40
Total	120

During the master phase I finished the following courses for astronomy: high energy astrophysics, basic detection techniques, star and planet formation, introduction to plasma physics, space mission technology, active galaxies, nuclear physics and subatomic physics. Adding to a total of 40EC.

As I was thinking about what I wanted to do for my internship, I realized that it would be useful to create a connection between the internship and my master thesis, to create a combined program. To the head of the educational program at that time (Prof. Dr. S. Trager), this sounded like an excellent idea. That's when I first heard about the Infoversum, a new full 3D dome theater to be build in Groningen. The Infoversum is founded by Prof. Dr. Edwin Valentijn, who is working at the Kapteyn Astronomical Institute. One of goals of the Infoversum will be to bring science in closer connection with the public. 'The science of today will be shown in the Infoversum today' is one of the philosophies at the Infoversum. An important part in realizing this goal is visualizing and communicating science in an understandable way.

As my interest lies in communication and visualizing science, it would be great if this could be part of my master thesis. My work might then be useful for the Infoversum in the future, as part of my internship or in another way. Since the Infoversum brings the opportunity to really do this in the future, I decided that I wanted to do the internship at the Infoversum and that I want to do master thesis in that context. So this thesis focuses on science, with the internship at Infoversum in the back of my mind. During the internship I will have to write an advise report addressed to the Infoversum, in which I will advice the company on their business and policy with respect to communicating astronomy to the public. This includes market analysis, cost-benefit analysis and multi-criteria analysis (MCA). An MCA is basically a cost-benefit analysis, but with the difference that the assessment criteria are criteria that can't be monetized. In this thesis I will make a simple MCA for a few surveys that have the potential of finding strong lenses. This gives the thesis a tiny SBP edge. So to emphasize once again, this thesis is worth half a study year, which is 30EC.

CHAPTER 1 Aim of the Thesis

Every new survey has a chance of discovering new gravitational lenses. The Kilo Degree Survey(KiDS) (de Jong et al., 2013), an optical survey done with the VST telescope at Paranal (Chile), is a relatively new survey which officially released their first data (DR1) recently (Jong, 2013). Based on previous surveys (Jackson, 2013) it is very likely that KiDS will also contain at least a few (unknown) gravitational lenses, so undiscovered gravitationally lensed quasars (QSOs) will probably be somewhere in the completed observations. The goal of this thesis is to explore the possibilities of finding unknown strong gravitationally lensed quasar (QSO) candidates in KiDS. We want to emphasize that the thesis aims specifically to find lens *candidates*, because KiDS is not expected to give an inconclusive answer about if a source really is a lens. Follow-up observations will be needed for that. To explore the possibilities of finding lens candidates, we first need to get a general of idea of what to expect of lenses in KiDS. Knowing how many lenses can be expected in KiDS, and how these lenses will look is an invaluable piece of knowledge we need to have before we can think of developing methods for finding them. Based on the things we learn in the first step, we want to come up with a few different methods of finding strong lens candidates, and test those methods to see how effective these methods are at finding lens candidates. We want to compare the developed methods against each other, looking at aspects like completeness, contamination and cost.

The thesis will also contain a small SBP part, as discussed in the prologue. We want to determine if KiDS is a good survey for finding lenses, compared to a few other surveys. For that we will use an SBP method called a multi-criteria analysis (MCA). All this work will finally result in an advise to the KiDS-team in which direction tehy should proceeded to efficiently start searching for unknown strongly lensed QSO candidates within KiDS. For finding strong lenses, KiDS is a perfect test case because it is a relatively small survey. This thesis aims not to be conclusive by all means, but it should at least give handles on next steps that have to be taken in order to start finding unknown gravitationally lensed QSO candidates in new observations. The results of this work can also be applied to other surveys in a more general sense, so it is potentially interesting for future surveys like Euclid, with a much larger sky coverage then KiDS. Surveys with a much larger sky coverage are expected to contain more strong lenses, and therefore need efficient methods to find the unknown lenses.

CHAPTER 2

Introduction

Before going deep into the candidate selection procedure, it is useful to have a general understanding about the subject of gravitational lensing. Gravitational lensing is everywhere, but strong gravitationally lensed QSOs are not very common. Because we can learn many interesting things from gravitational lenses, every new found lens is potentially interesting for scientists. Gravitational lenses can be used to study large scale structure and calculate cosmological parameters like H_0, but can also be useful for deriving properties of the lensing galaxy or the source that is observed (Jackson, 2013).

In this introduction the phenomenon of gravitational lensing is discussed in greater detail. A description of the KiDS survey is given, as well as some background on the Astro-WISE information system, which has an essential roll in this project.

2.1 Gravitational Lensing: What Is It?

2.1.1 Basic Concepts

General relativity states that under influence of a mass the space-time continuum is deformed, bending space and time locally (see Figure 2.1). Following this theory, a photon locally gets deflected by an angle:

$$\theta = \frac{4GM}{c^2 R} \tag{2.1}$$

in which G is the gravitational constant, M the mass of the object, the speed of light c and the radius of the object, R(Kembhavi and Narlikar, 1999). The light is bent in the direction of the mass, making the mass actually act as a lens in space. The concept of a 'gravitational lens' was born. Since photons can be bent at any side of the lens, multiple projections of a single source becomes possible. In theory every mass in the universe acts as a lens, but depending on the mass the object causes a different deflection angle of the photons, which leads to different effects. The effects can be divided into three main categories: strong-, weak- and micro lensing. Strong lensing is the effect of a large mass over long distances, causing the appearance of multiple projections of the same object. Weak gravitational lensing is caused when the mass of the lens is not large enough to cause multiple images of the same source. Instead a background source is simply deformed or stretched. Micro-lensing is the effect of smaller masses on light received from a source. For instance, light of sources might be amplified for a short time because a large mass is passing in front of it. The effect is so small that it is invisible to the eye and only statistically measurable.

In 1919 Eddington first observed this effect by seeing the position shift of stars close to the sun during a solar eclipse. It was not until 1979 before the first real strong gravitationally lensed QSO system was observed (Jackson, 2013; Walsh et al., 1979). Most gravitational lenses in that period where discovered with radio surveys, but since 90% of all QSOs have no bright radio emissions, the search for radio quiet QSOs began soon afterwards. Optically lensed QSOs began to be discovered not long after that.

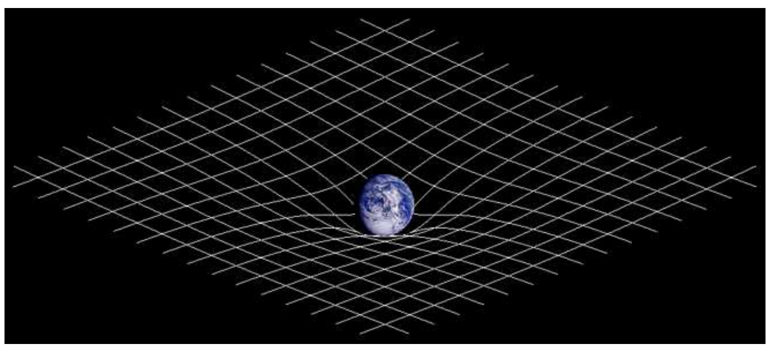

Figure 2.1: Impression of space-time curvature that is caused by a mass, in this example the earth (http://physics.stackexchange.com.

From formula 2.1 follows that for strong lensing to occur, the mass of the lensing object has to be large and confined to a relatively small area(Kembhavi and Narlikar, 1999). This makes galaxies and clusters of galaxies excellent candidates for strong gravitational lensing of QSOs. Most of the lensing galaxies in strong gravitational lens systems turn out to be early type elliptical galaxies, because they are more massive than other types of galaxies in general (Jackson, 2013). In Figure 2.2 we see an impression of the effect of strong gravitational lensing. More on this in the next section.

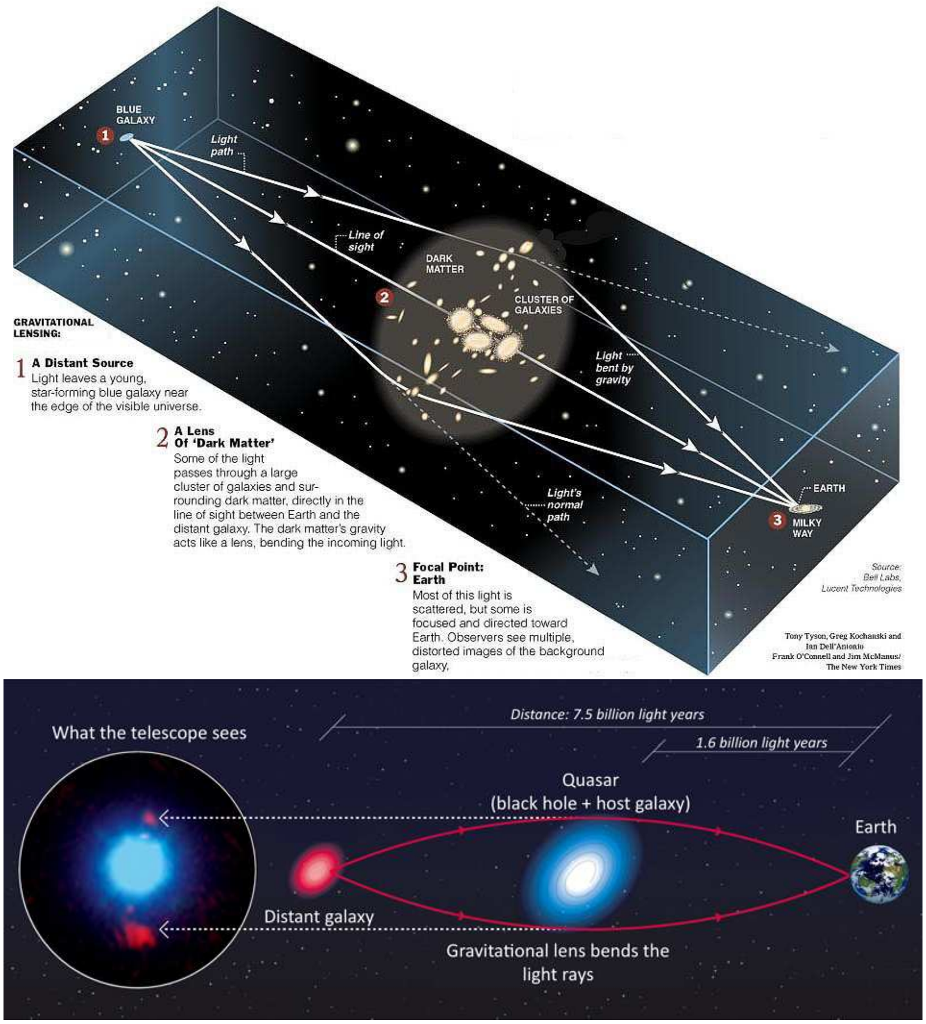

Figure 2.2: Impression of the theory behind gravitational lensing. Light from a distant source gets deflected towards the observer due to a point mass between the observer and source(top image:http: www//lsst.org and bottom image:http://www.astro.caltech.edu).

Another interesting consequence of gravitational lensing is that magnification of the source can occur. Details of this mechanism are not part of this thesis. However, the magnification effect is potentially very interesting because it makes detailed study of the lensed source possible. Also objects that are fainter than the theoretical limiting magnitude of a certain telescope, can become detectable because of the amplified light. We now delve deeper into the subject of strong gravitational lensing, since this is the focus of this thesis.

2.1.2 Strong Lensing

When the observer, the lens and the lensed source lay exactly or almost exactly in one line, and the lens itself is very massive, the light can take multiple paths around the lens to the observer. As a result one can see multiple images of the same source around the lens. In most cases we see 2 images (doubles), sometimes 4 (quads) or even more in extreme cases (which is very rare). See the bottom image of Figure 2.2 for an impression of how lensing works. The appearance of multiple projections is a consequence of the properties of the lens Fermat surface Jackson (2013). Typical separation of the different images of the same source with respect to the lens are in the order of a few arcsec. See Figure 2.4 for the estimated distribution of separations for galaxy, group and cluster lenses. When clusters act as a lens, the separation can become very large. Separations of up to 20" or even more are possible, but are very rare (Jackson, 2013).

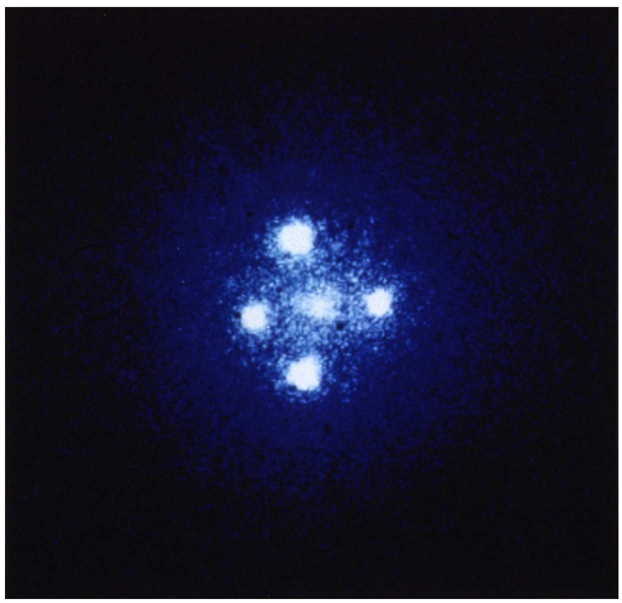

Figure 2.3: Picture of the quad lens G2237 + 0305 quad lens, a gravitationally lensed quasar. The typical composition of a quad lens is also known as an 'Einstein cross' (source: HST).

An important advantage of multiple images of the same source is, that they can be used to study the expansion of the universe. Source like QSOs and SNe are in many cases variable over time. Since the photons of image of the QSO take different paths through space, these variations in brightness arrive at different times to the observer. Because the events happened only at one time at the actual source, the observed time delay can be used to study shape of space-time between the source and the observer. One can for instance calculate the value of the Hubble constant, H_0, using time delays.

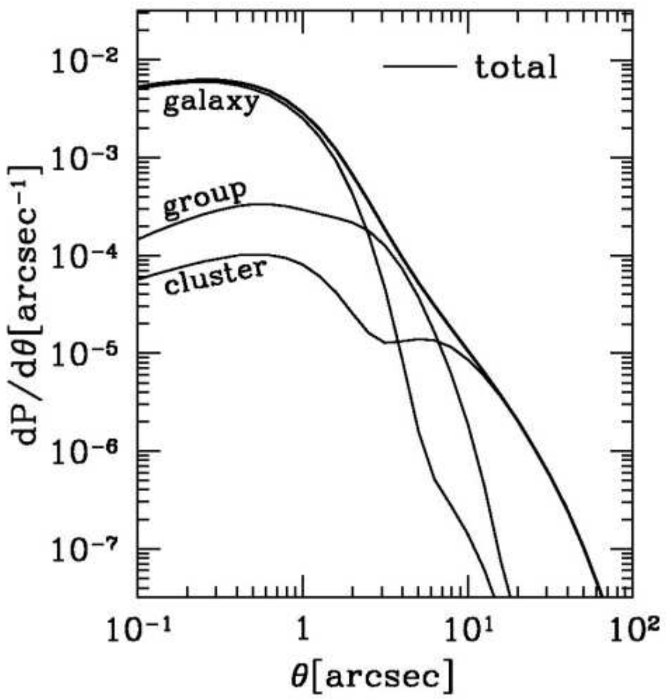

Figure 2.4: The distribution of lens image separations for three different scales: galaxy, group and cluster scales. Distribution is predicted by a halo model (Oguri and Marshall, 2010).

When the observer, lens and source are exactly aligned, the projection of the source can be such that the observer will see a so called 'Einstein ring'. More often than a ring, the source may get stretched out and curved, and form a tangential or radial arc. A lot of mass is necessary for arcs to appear, so the properties of the arc can be used to study the mass distribution of the lens for instance. An example of an Einstein ring is shown in Figure 2.5.

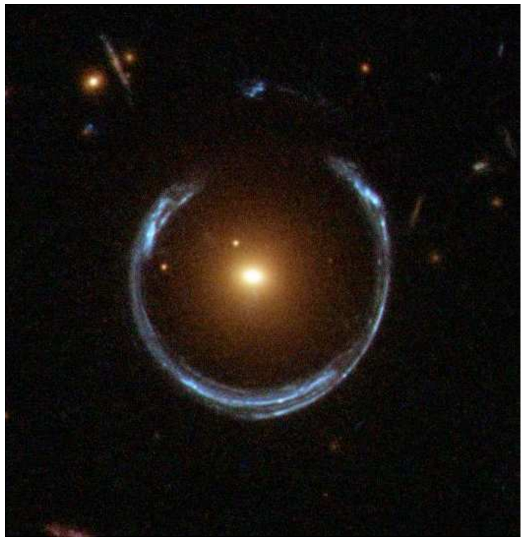

Figure 2.5: Example of an Einstein ring, called the Horseshoe (source:Hubble).

Typical Lenses

Very massive objects cause strong gravitational lensing. Galaxies are thus good candidates for gravitational lensing. Galaxies come in many different shapes and sizes, but in general early type galaxies (red ellipticals) are more massive than any other kind of galaxy. Therefore early type galaxies are the most common lenses in the universe. In practice $\sim$80 % of all lenses are ellipticals, so they dominate the lensing cross section (Turner et al., 1984). But still there are a significant 20% of other lens types left.

This 20% consists of late type spirals and any other type of galaxies, but groups and clusters of galaxies cause most of the residual lensing observed. Because these groups/clusters contain multiple galaxies, their mass as a whole is huge. Because of the mass and spatial size, separations of the images of the sources are much higher than those of single galaxy lenses, sometimes up to 20".

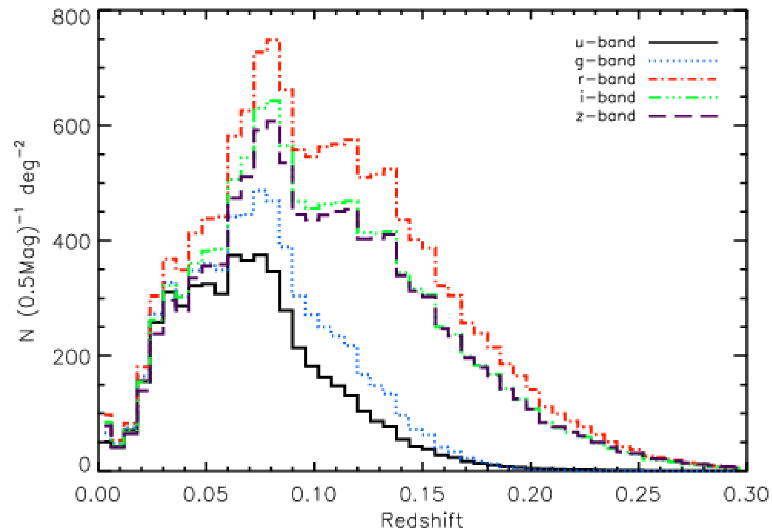

Figure 2.6: The distributions of galaxies versus redshift up to 0.3 in all filters of SDSS DR6.

Most galaxies in the universe reside at a redshift between 0 and 1 (see Figure 2.6). This means that many lenses will be in this redshift range, which consequently means that lensed sources will have to be at a higher redshift to be able to be lensed.

For cluster/group lenses it is hard to determine if the images are from the same source. You will need for instance spectroscopic data to determine if the redshifts of the images are the same. If they match it could be a cluster scale gravitational lens.

Typical Lensed Sources

Since lensed sources are even further away than the lenses, the source should be quite luminous. Otherwise you could never observe the source, and you would never see it was lensed. Since galaxies are the most common large massive luminous objects in the universe, most lenses are galaxy-galaxy lenses. The lensed galaxy will typically be somewhere between redshift 0 and 2. When the galaxy is very luminous, the lensed galaxy can even be at a higher redshift.

Beyond a redshift of 2 there are not many sources that can be lensed, because they become too faint. Only extremely luminous sources are left. There are only a few types of sources that are so luminous that they still can be observed at high redshift. The most luminous objects in the universe are QSOs and supernovae. Since QSOs are more common than supernovae, and shine for 10^{7-8} years instead of several days to weeks, lensed QSOs are much more likely to be observed.

Quasars

The central region of a galaxy consists in most cases of a bulge with a supermassive black hole in its center. The bulge is basically a dense cloud of gas around the black hole. Material in this region is constantly rotating at high speed, and falling into the black hole. This causes the gas to heat up and the gas starts emitting photons. From earth we observed a really bright active galaxy, which we call a quasar (QSO). In most cases we observe a QSO as a point source on the sky, since the emission of radiation is only from the central region of the galaxy, and thus coming from a very small confined region.

In extreme cases the central black hole cannot keep up with the speed of accretion, and massive amounts of energy get blown out into space at incredible speeds (sometime close to the speed of light). We call this a (superluminal) jet. A jet is incredibly strong collimated beam of high energy radiation emitted from a black hole or star (see Figure 2.7 for an impression). When we look exactly or almost exactly in the beam of the jet emitted by this galaxy, we also see a very bright source.

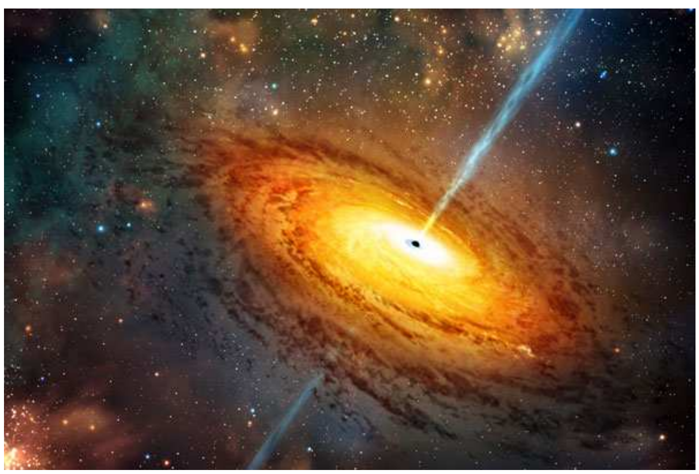

Figure 2.7: Impression of a galaxy with a very powerful jet emitted from its central black hole. When we look into the jet, as seen from earth, we call that object a quasar.

Since QSOs are so bright, we can find them at much higher redshifts than normal galaxies. In Figure 2.8 we see the distribution of QSOs with redshift in SDSS DR7 and DR9. We can see that QSOs have a typical redshift between 0 and 4, and it peaks around z= 2. The dip in the DR9 line is caused by different selection criteria for QSOs. QSOs are on average at a higher redshift than lensing galaxies. Therefore they are excellent candidates to be lensed by a galaxy at lower redshift. In practice 1 in ∼500 to 1 in ∼1000 QSOs are lensed (Schneider et al., 1999).

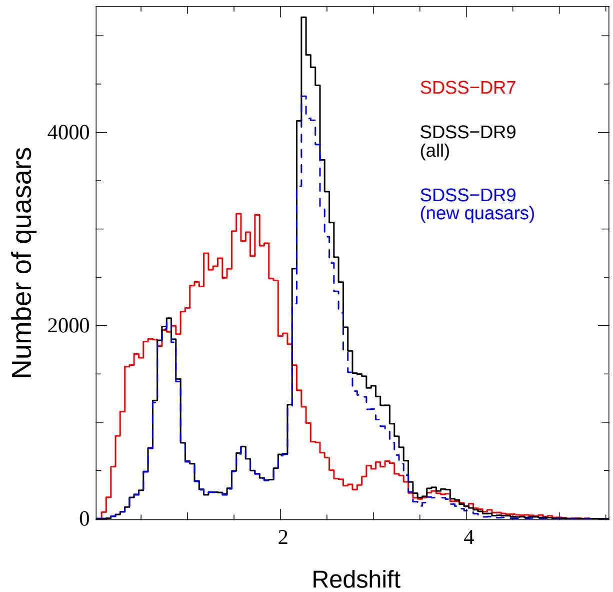

Figure 2.8: The distributions of QSOs versus Redshift in SDSS DR7 and DR9 (Pâris et al., 2012).

2.1.3 Status of the field

The field of gravitational lensing is running since the 70's. There are about 650 gravitational lens systems discovered so far. The CLASS radio survey (Browne et al., 2003; Myers et al., 2003) is the largest systematic radio survey, and it produced 22 lens systems. More information can be found at http://www.jb.man.ac.uk/research/gravlens/class/class.html. After observations of QSOs in the optical regime became available in substantial numbers by SDSS, sub-sequential lens searches like the Sloan Quasar Lens Search(SQLS) produced about 30 lensed QSOs (Oguri et al., 2006; Inada et al., 2012). An overview of the SQLS lenses can be found at http://www-utap.phys.s.u-tokyo.ac.jp/~sdss/sqls/lens.html.

Sloan Lens ACS (SLACS) and the CfA-Arizona Space Telescope LEns Survey (CASTLES) are examples of follow up observations on known gravitational lenses. With the high resolution images of HST detailed study of the lenses becomes possible. More information about these projects is available at http://www.slacs.org/ and http://www.cfa.harvard.edu/castles/

The most complete database of strong gravitational lenses currently is the Masterlens project (www.masterlens.org), which is a merging of the catalogs discussed before plus many more lenses detected. In total there are about 120 strong gravitationally lensed QSOs known. More on the masterlens database in section 5.2.

2.2 KiDS

2.2.1 General Survey Description

KiDS, short for the Kilo-Degree Survey, is a large-scale optical imaging survey taking place at the ESO Paranal observatory, Chile. Observations started on October 15th, 2011 and are ongoing. KiDS is developed to give answer to a few fundamental questions of cosmology and galaxy formation today. Using the OMEGAMCAM at the VLT Survey Telescope (VST) KiDS will observe ∼1500 square degrees of the night sky in four different filters (u, g, r, i), which are similar to the SDSS filters. The central wavelengths of the filters are summed up in Table 2.1, together with the seeing statistics per filter. All observations consist of five visits, all made right after each other (de Jong et al., 2013).

Table 2.1: Overview of all KiDS filters, their central wavelengths, 5σ limiting magnitude, seeing and exposure time (de Jong et al., 2013).

Filter	Central Wavelength [nm]	Limiting Magnitude	average FHWM(PSF)	Total Exp time. [s]
u	350	24.4	1.0	900
g	480	25.1	0.8	900
r	625	24.9	0.7	1800
i	770	23.7	0.8	1080

2.2.2 Survey Fields

The KiDS surveys consists of two separate fields, one in the northern(KiDS-N) and one in the southern sky(KiDS-S). Together they make up a total of ∼1500 square degrees. The fields are explicitly chosen to overlap with previous surveys, like the 2dF and SDSS survey, which also had a focus on observing the redshift of a large number of sources. It also helps because these surveys give a good map of the foreground galaxy distribution out to a redshift of ∼0.3. One of the most important aims of KiDS is to 'weigh' these galaxies systematically as function of their type and environment(de Jong et al., 2013).

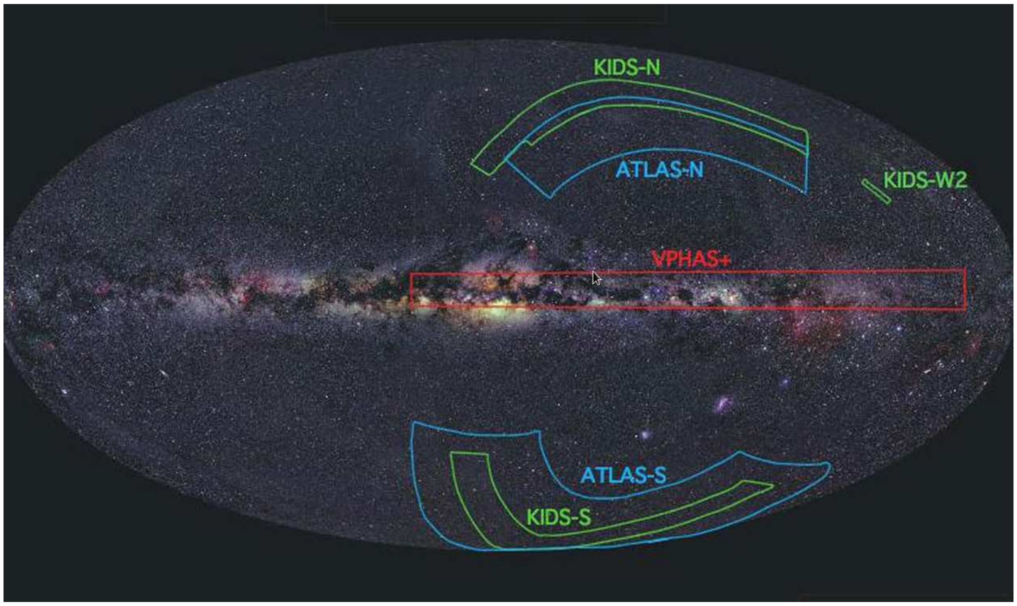

Figure 2.9: The kids field relative to the Milky Way plane. (source:http://www.eso.org)

2.2.3 KiDS-ESO-DR1

Recently, the first public data release of KiDS (KiDS-ESO-DR1) has become available (Jong, 2013). DR1 consists of the first 50 square degrees that were successfully observed in all filters. With this release come calibrated stacked images and their corresponding weight frames, but also masks and single-band sourcelists belonging to the stacks. The data is available via the ESO archive facility, as well as via the Astro-WISE Information System.

2.2.4 General Survey Progress

KiDS observations are ongoing. In total a number of 1500 tiles are going to be observed during the whole observation period (2011 - ∼2016). Recently, KiDS has delivered their first data release (DR1) to ESO. Internally there is already more data available, and currently the number of completed tiles lies around ∼150. In Figure 2.10 the position of all observed tiles up to 24-1-2014 are shown. More information and a daily updated overview of finished tiles can be found at the wiki page: http://wiki.astro-wise.org/projects:kids:survey_progress:survey_progress.

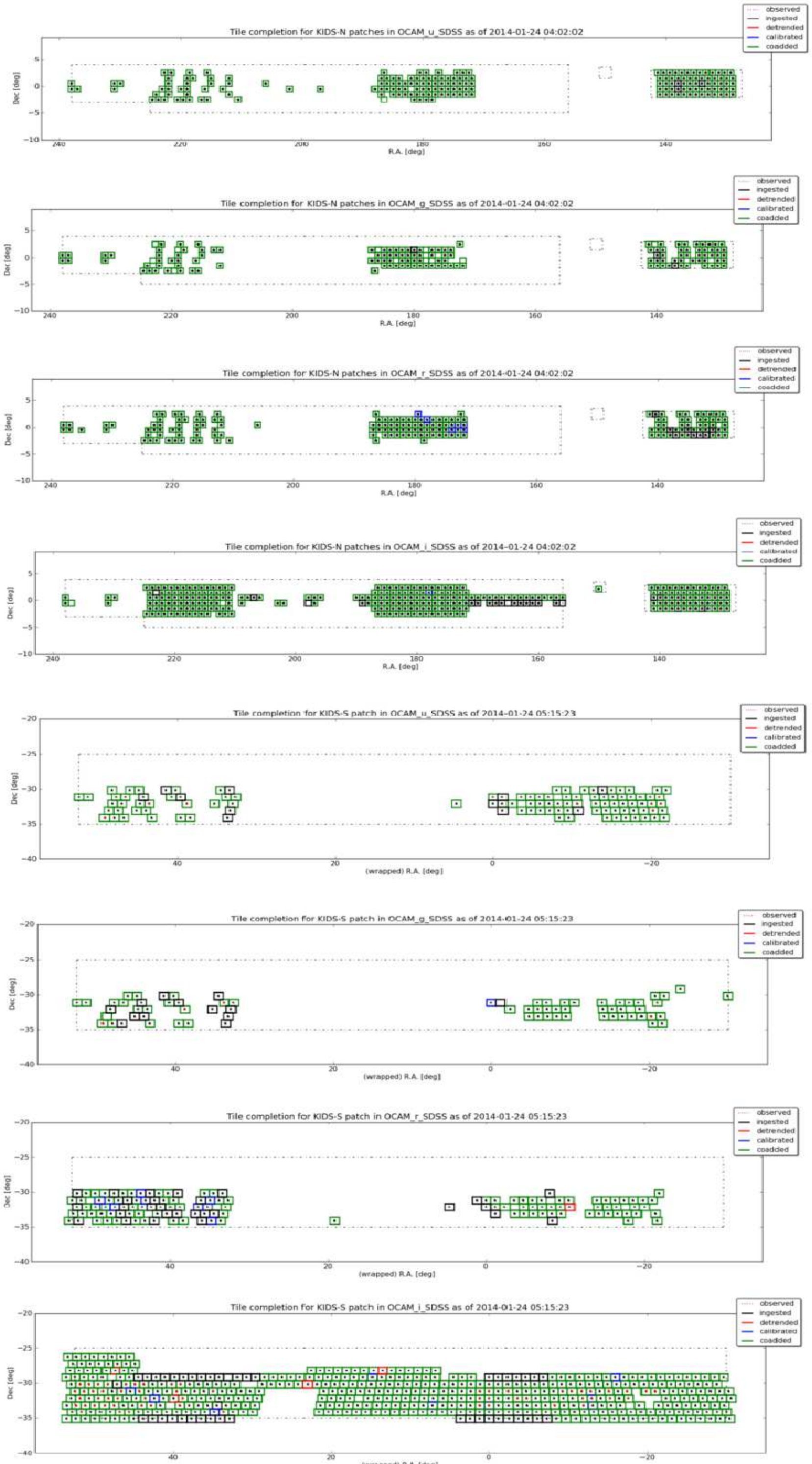

Figure 2.10: Survey progress of the KiDS-N and KiDS-S fields up to 24th of January 2014 in all 4 color bands (source:http://www.astro-wise.org.

2.2.5 OmegaCAM

The VST at Paranal has a state of the art 2.6m telescope at its heart. This telescope is equipped with a 32-ccd, 268-megapixel camera called OmegaCAM. It's instantaneous field of view is a full square degree, which is mapped at 0.2 arcsec/pixel, sufficient to sample even the best seeing images possible on Paranal. For KiDS, OmegaCAM uses 4 filters (u, g, r and i), which are broadband filters similar to those of SDSS. This means KiDS operates in the optical regime of the electromagnetic spectrum (de Jong et al., 2013). Image quality, reliability and throughput are all maximized. See Figure 2.11 for the PSF of KiDS. The combination of excellent natural seeing at the site and fully active optics in the telescope let OmegaCAM make the most out of the observational circumstances at Paranal (Kuijken, 2011; Verdoes Kleijn et al., 2013).

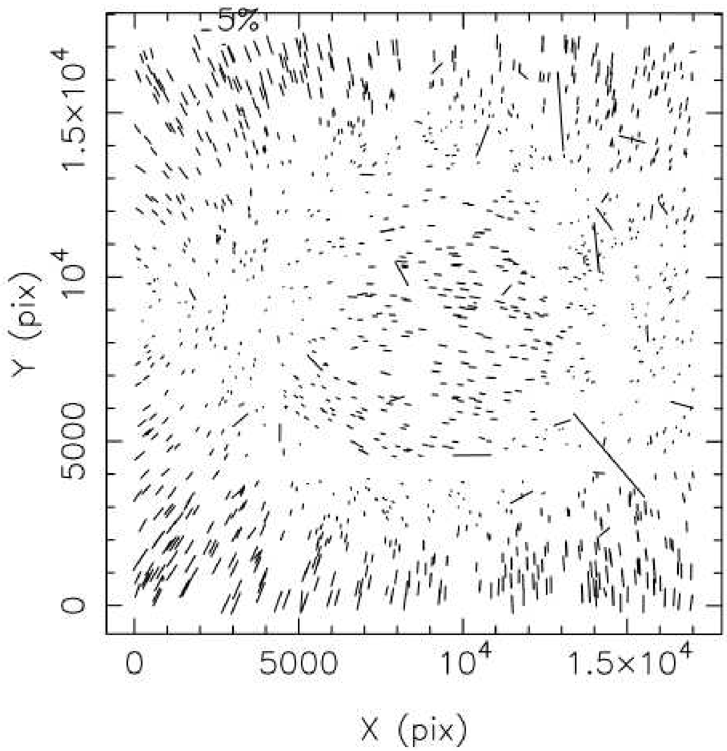

Figure 2.11: The point spread function of OmegaCAM, unmatched by other wide-field cameras available existing today http://wiki.astro-wise.org/.

2.2.6 Scientific Goals

In this thesis we are exploring a new scientific goal for KiDS. Strong lensing was not part of the official ESO proposal and did not drive the survey design. The original scientific goals of KiDS are described in detail in the survey description by de Jong et al. (2013). Details of all the scientific goals will not be discussed here, but a short description follows.

The main target of the KiDS survey is mapping the matter distribution of the universe through weak gravitational lensing and photometric redshift measurements. Another target for KiDS is to understand more about the inner regions of galaxy halos, and in that way learn more about the structure of galaxy halos in general. With a median redshift of $\sim$0.8, KiDS will have a real good sample of galaxies to study galaxy formation and evolution processes in great detail. Since KiDS data is deeper than SDSS, the data can also be used to study the Milky Way in higher detail than is done with SDSS data earlier, especially to look for stellar streams.

2.3 Data in this project

For this project we use or combination of KiDS-ESO-DR1 plus KiDS-INT-DR3. KiDS-INT-DR3 is the internal release of completed data, that are not officially released, but are ready to use. It comes down to a total of $\sim$159 tiles (each approx. 1 sq.deg.) for which u, g, r and i band observations are available. Positions of all tiles are shown in Figure 2.12.

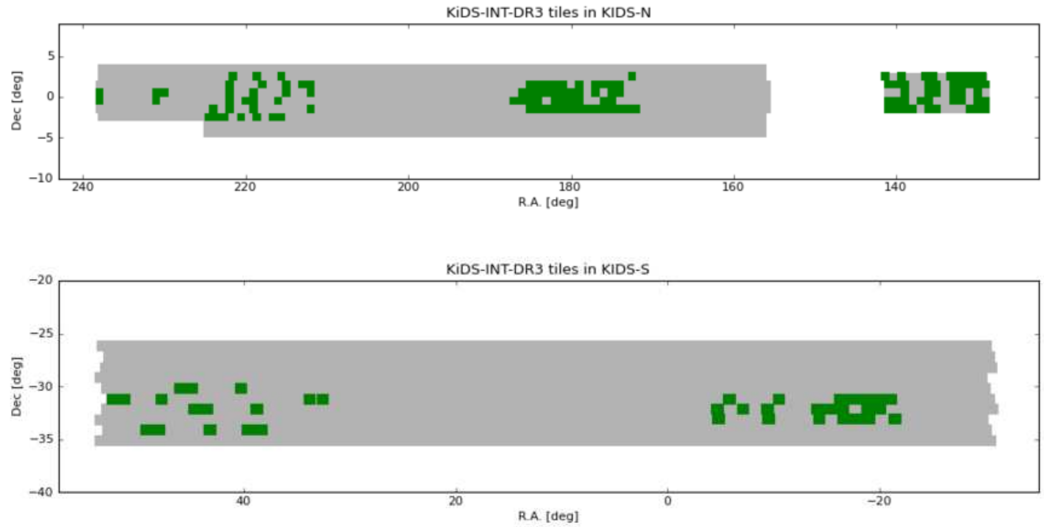

Figure 2.12: Overview of the position of the field used in KiDS-ESO-DR1 and KiDS-INT-DR3 http://wiki.astro-wise.org/.

For this project we have used only calibrated co-added data. Co-added data are built up out of 4 (u) and 5 (g,r,i) stacked, dithered exposures. Calibration is done using Global Astrometry. Global astrometry is the best quality astrometric solution obtained by the KiDS survey pipeline (see de Jong et al. (2013) for details on KiDS observations and McFarland et al. (2013a) for more on Astro-WISE quality control.). It obtains a single astrometric solution using the overlapping sources between exposures, plus 2MASS as astrometric reference catalog (see McFarland et al. (2013b) for image pipeline details).

If we compare the Sloan Digital Sky Survey (SDSS) to KiDS, we see that KiDS overlaps partially with SDSS (SDDS has a coverage ∼20,000 square degrees). However, KiDS goes deeper by about 2 magnitudes, and it has better image resolution, particularly in the g and r-band.

2.4 Astro-WISE

For dealing with the astronomical data KiDS produces overnight, a consortium built a system called Astro-WISE. The name Astro-WISE stands for Astronomical Wide-field Imaging System for Europe. The system has been developed to do the processing of the data is well as the management. Astro-WISE is an environment consisting of hardware and software spread out over several institutions in Europe, and was originally specifically developed to process data from the Omega-

CAM wide-field camera on the VST. Astro-WISE allows a scientist to work with raw data, calibrated data, perform analysis with it and finally archive it as well. Based on an underlying data dependency tree, the system brings all steps of the processing chain together (see Figure 2.13).

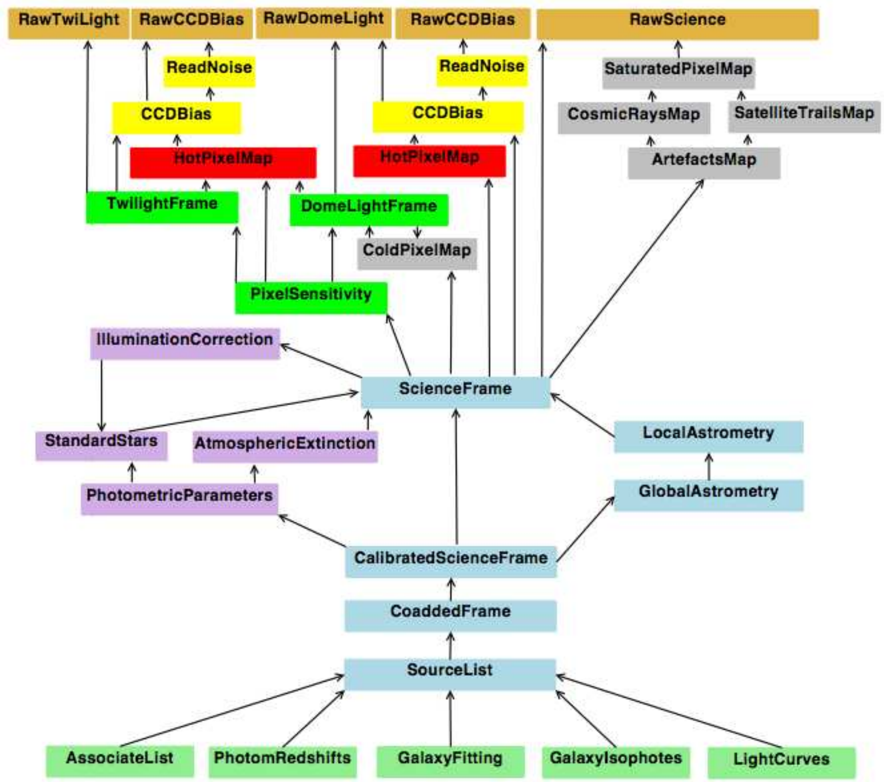

Figure 2.13: The dependency tree of KiDS-data within the Astro-WISE information system (McFarland et al., 2013b).

Users can interact with the Astro-WISE system via a command-line interface, which also allows them to write their own scripts and methods or make changes in the code of their own check-out of the software. This makes it possible for all users to help improve the system and collaboratively work on new versions of the pipeline. Apart from the command-line interface there are also several web-interfaces available: for example a database viewer (http://dbview.astro-wise.org/), a calibration data management system and a data processing interface to produce advanced data products in one go. This system allows users in any location to have an up-to-date overview of all available data, and to use hardware in any location to work on survey production. It's possible to work with Astro-WISE using the CVS file management system. Finally also a wikipedia page (http://wiki.astro-wise.org/) is used to keep track of projects and work done by various scientist. For more information on Astro-WISE you can visit the Astro-WISE website http://www.astro-wise.org/.

2.4.1 The Astro-WISE Dependency Tree

The rapid increase in the amount of data obtained during observations demands a new approach in handling data fast and efficient. This is important for using the data as well as checking the quality of it. To do science with the data a scientist needs a system for accessing the data (pixels) as well as as much information as possible about the data (metadata) at any stage of the process. Astro-WISE has fully integrated data lineage with backward chaining. Detailed description of this system is too much for this thesis, but a few important concepts will be discussed.

The steps from raw data to the final data consist of a few main steps. You can see the steps in Figure 2.13. Data is pulled from the system via the command-line. At the right top side you see that the raw observations convert to a rawScienceFrame. After correcting for hot/cold pixels, flatfield and bias one is left with a ReducedSienceFrame. With the help of astrometric parameters a RegriddedFrame is constructed, which means all coordinates are set correctly for a chosen coordinate system. After that all the frames only have to be stacked to form a CoaddedRegriddedFrame. From the CoaddedRegriddedFrame a SourceList and AssociateList is created, and then the tile is ready for scientific research (McFarland et al., 2013b).

CHAPTER 3

Expected Number of Strongly Lensed Quasars in KiDS

3.1 Introduction

Before we will be starting to look for new strongly lensed QSOs in KiDS, it is useful to know as accurately as possible how many strong lenses can be expected in KiDS. Based on that number we can decide if it makes sense to search for them at all. In 2010, Oguri and Marshall published a paper on the subject of strongly lensed QSO predictions in upcoming surveys (Oguri and Marshall, 2010). KiDS was not discussed in this paper, but their method is useful for deriving an estimate for KiDS as well.

3.2 Deriving the Expected Number of Strongly Lensed QSOs in KiDS

The goal of the paper of Oguri and Marshall (2010) is to derive estimates of expected number of strong gravitational lenses for the Large Synoptic Survey Telescope (LSST) and several other surveys. They also aim to create a mock catalog of strong gravitational lenses, which can be used to investigate the feasibility of various science projects. Using a few formulas, of which we will not go into detail here, they integrate the lensing cross section of each galaxy over the galaxy population and redshift range (e.g. Turner et al. (1984)). They use QSOs and supernovae (SNe) as sources. When you combine the population of lensing galaxies and the number density of lens sources, you can determine how many strong lensing will occur. See Figure 3.1 for the calculated lens and source distributions. This all depends on depth and resolution of the survey. In the next step they give an overview of several surveys and their expected number of strong lenses. Oguri and Marshall did their calculations specifically for theoretical i-band observations of LSST, a new survey to be built in the near future. But the theory can be used for any kind of survey, if you know its characteristics like limiting magnitude and sky coverage.

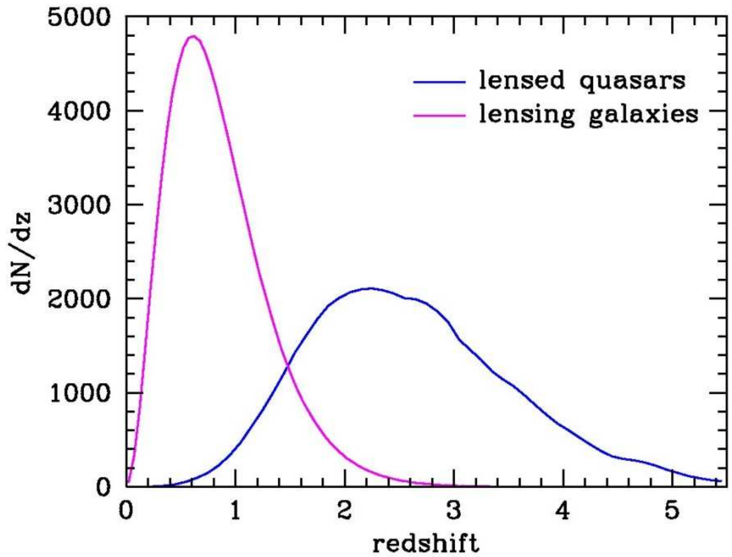

Figure 3.1: Approximated redshift distributions of lensed QSOs (blue) and and lensing galaxies (magenta) adopting i_{lim}=24 for LSST (LSST, 2009).

In Table 3.1, which is the same as table 1 in Oguri and Marshall (2010), an overview over several surveys are given with their respective area, limiting magnitude in the i-band (per visit, per year and total), resolution, cadence and running time. For KiDS the corresponding i-band and r-band data are added to the table. Because the magnitudes used by Oguri are 10σ point source limiting magnitudes, and the magnitudes of are KiDS 5σ limited, the KiDS magnitudes need to be converted to match the Oguri and Marshall magnitudes.

Table 3.1: Selection of surveys and statistics from table 1 of the paper of Oguri (2010). Magnitude are 10σ point source limiting magnitudes. KiDS-i and KiDS-r are added to this table (Oguri and Marshall, 2010)

Survey	Area [deg^2]	$M_{i,lim}$ (visit)	$M_{i,lim}$ (year)	$M_{i,lim}$ (total)	θ_{PSF} [arcsec]	cadence [days]	T_{survey} [years]
KiDS-i	1500	23.0	23.0	23.0	0.8	-	5
KiDS-r	1500	24.2	24.2	24.2	0.7	-	5
HSC-wide	1500	24.3	24.9	25.5	0.75	-	3
HSC-deep	30	25.3	24.9	25.5	0.75	5	3
SDSS-II	300	21.3	22.9	23.5	1.4	5	3
PS1/3π	30000	21.4	22.2	22.7	1.0	30	3
DES-wide	5000	23.6	24.0	25.1	0.9	30	5
DES-deep	6	24.6	26.1	27.0	0.9	5	3
JDEM/SNAP	15	27.1	-	29.7	0.14	4	1.3
LSST	20000	23.3	24.9	26.2	0.75	5	10

The 5σ limiting magnitudes for KiDS are already given in Table 2.1. For i this is ~ 23.7. Because KiDS only visits every patch at the sky once, the maximum depth of KiDS is reached immediately, and thus the total magnitude is consequently the only magnitude relevant. Assuming that the source noise is much smaller than the sky noise, which is the case for the observation of very faint sources, we can use equation 3.1 and 3.2 (Patat, 2003). A 10σ limiting magnitude means a signal to noise ratio (SNR) of 10. For 5σ the SNR is 5.

$$\frac{S}{N} = \frac{P_{source} \cdot T}{\sqrt{(P_{source} + P_{sky}) \cdot T}} = \frac{P_{source}}{\sqrt{P_{source} + P_{sky}}} \cdot \frac{T}{\sqrt{T}} \tag{3.1}$$

$$\frac{(\frac{S}{N})_{=10}}{(\frac{S}{N})_{=5}} \approx \frac{P_{source,10}}{P_{source,5}}; P_{source} << P_{sky} \tag{3.2}$$

To calculate the 10σ limiting magnitude, we use equation 3.3, where M_x and P_x are the magnitude and power (flux) of the source you want to calculate, and $M_{x,0}$ and $P_{x,0}$ are a reference magnitude and flux. From formula 3.2 it follow that the flux ratio$\frac{P_{source,10}}{P_{source,5}}= 2$, and $M_{x,0}$ can be put to 23.7. The 10σ corrected limiting magnitudes for i becomes 23.0.

$$M_x - M_{x,0} = -2.5log_{10}(\frac{P_x}{P_{x,0}}) \tag{3.3}$$

In Figure 3.2 the number of expected lenses is plotted against potential limiting i-band magnitude for the LSST (20000 deg^2). We use this plot to make an estimate for KiDS, by reading the value at a limiting magnitude of 23.0, and correcting the number from 20000 deg^2 to 1500 deg^2 for KiDS.

For the i-band, the number of lenses we find is $\sim$ 200-225. So assuming that what Oguri and Marshall did is close to reality for the i-band, it's fair to say that the estimated number of strong lenses in KiDS will be somewhere between 200-225. Since almost 8% of all tiles are part of this thesis, we can expect to find 15-20 lenses in the i-band data we analyze in this thesis.

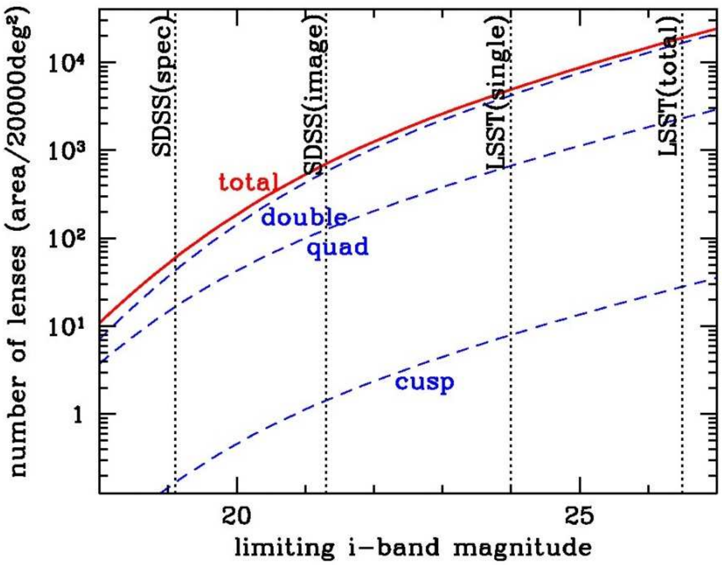

Figure 3.2: The number of lenses expected in a 20,000 deg^2, as a function of Limiting i-band magnitude. ashed lines are numbers of lenses for each image multiplicity (double, quadruple, and three-image naked cusp lenses). The total number is indicated by the red solid line. Limiting magnitudes in SDSS and LSST are shown by vertical dotted lines. Using this plot and i_{lim} = 23.0 we find N_{lens}=225 for KiDS (LSST, 2009).

Because we know that the limiting magnitude and seeing of KiDS are the best in the r band, it might be useful to also calculate the expected number of lenses based on r, because that number might be different, and is expected to be higher. But because the expected number is based on i-band, we need to correct the r-band limiting magnitude to an i-band magnitude, before we can use it consistently.

In Figure 3.3 a model of the r-i magnitude of QSOs and ellipticals is plotted against redshift. We see that for QSOs the r-i magnitude is, on average, 0 over the entire redshift range. This is expected because a QSO spectrum is known to be more or less flat in the optical regime. So if we want Figure 3.2 to calculate the number of lenses detected in the r-band we can use the limiting magnitude of the r-band with no correction needed. So we can use 24.9 as limiting magnitude (see Table 2.1). We still need to correct for the 5σ to 10σ difference, which is done using the same approach as for the i-band. So we finally use 24.2 as number to calculate the number of lenses expected in r. Using Figure 3.2, we estimate the number of lenses in the r-band will be about ∼450, which is double the number for the i-band. So assuming this method is close to reality, the number of expected lenses in KiDS lies somewhere between 200-450. In the available data this comes down to 20-50 lenses.

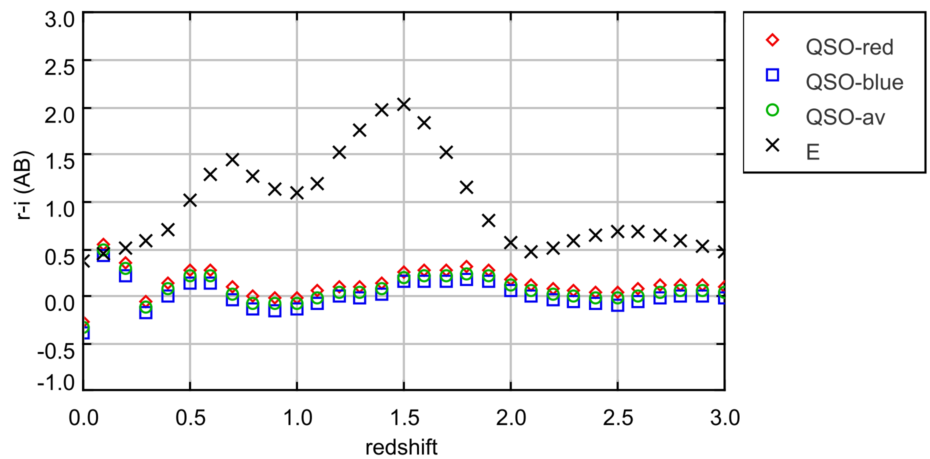

Figure 3.3: Model of typical r-i magnitudes for QSOs and Ellipticals (Kembhavi and Narlikar, 1999).

The number of strong lenses expected for all the surveys discussed in Table 3.1 is given in Table 3.2. KiDS is now added to the list. LSST is clearly the survey with, by far, the highest number of lenses expected to be found.

Table 3.2: Expected number of strong lensed QSOs in the surveys of Table 3.1 (adopted from table 2 of Oguri and Marshall (2010)). The number of lenses expected for the KiDS i-band and KiDS r-band are added as well.

Survey	N_{lens}
KiDS-i	225
KiDS-r	450
HSC-wide	614
HSC-deep	30
SDSS-II	26
PS1/3π	1963
DES-wide	1146
DES-deep	4
JDEM/SNAP	22
LSST	8191

Oguri and Marshall concluded in their paper that survey area is more important than survey depth when it comes to finding lenses. Consider for instance that you find N lenses in one field within time T. If you double the field area you will find 2N lenses in a observing period of 2T. If you would not pick a different area, but integrate 2 times longer on the same field, you will reach 0.75 magnitude deeper in your observation. If you would do this at the depth of KiDS i-band you would reach a magnitude of 23.7. Then N_{lens} is $\sim$ 300 which is only a factor $\sim$1.3N higher. Going deeper in the same area does clearly not outweigh extending your observing area, if you want to find more strong lenses. This is an important thing to keep in mind.

CHAPTER 4

Mock Strongly Lensed Quasars for KiDS

4.1 Introduction

In the paper Oguri and Marshall (2010) also created a mock catalog of strongly lensed QSOs. With the paper comes a piece of software (which can be found online at https://github.com/drphilmarshall/OM10) to make your own mock catalog. Within this program you can enter an area, i-band limiting magnitude and minimum seeing value, to create your own sample of strong lenses corresponding to the characteristics of your survey. Since KiDS also has an i-band filter, this software can be used for KiDS as well. All kinds of parameters like z_{lens}, z_{source}, magnitude of all QSO images and the lens, image separations and much more information is given per individual lens in the catalog. This information is very useful for getting a picture of what can be expected in the survey, and testing the feasibility of science projects like finding strong lenses with certain surveys. For getting a feel of the kind of characteristics that potential lenses in KiDS will have, we will analyze our own mock sample.

4.2 The KiDS Mock Catalog

The approach Oguri and Marshall used to create the mock catalog is as follows. First they generated random realizations of lens and source distributions using Monte-Carlo methods. Using these distributions and solving the lens-equations for the positions, a mock strong lens catalog is produced. In Figure 3.1 these source and lens distributions were already shown. For multiple imaged sources it's checked whether they satisfy detection criteria (limiting magnitudes, image separations and flux ratio). Only lenses which survive these criteria are selected. The total number of strong lenses in the mock catalog is 3132 for lensed QSOs and 122 for lensed SNe. For more information on how they made the catalog, I recommend anyone to read the paper.

4.2.1 KiDS Mock i-band Statistics

For making the mock catalog for KiDS we use the i-band limiting magnitude and seeing from Table 2.1, with the 10σ corrected magnitude discussed in section 3.2. These value are 23.0 and 0.8 arcsec respectively for magnitude and seeing. The KiDS i-band specific mock-catalog consists of 188 lensed QSOs, which is a similar number as we found in the previous section. In Table 4.1 we show an overview of some average statistics of the mock lenses in the i-band. Average separation of the two brightest QSO images is ~1.6 arcsec. 13%(24) of the lenses are quads in this sample. Average redshift of the lens is 0.8, while the average redshift of the source is 2.45. The averages are interesting, but keep in mind that there is quite a spread in values, with maybe some extreme outliers influencing the average values.

Table 4.1: Some important statistics from the Mock lenses selected for KiDS i-band. Area=1500 deg^2, I_{lim}=23.0, PSF(FWHM)=0.8.

Parameter	Average
N_{lens} (QSO)	188
N_{quads}	24
$N_{doubles}$	164
Separation (two brightest images)	1.6 [arcsec]
z_{lens}	0.8
z_{source}	2.45
Apparent magnitude of lens	20.9

In Figure 4.1 we see the distribution of image separations of all the KiDS mock lenses. It's important to realize that in this case the separations means the separation between the two brightest QSO images (and not between the lens and the furthest image). We can see that the separations vary between 0.5 and 4.0 arcsec max. Most of the separations are centered around 0.5 - 2.0. About 20% of the image separations are below the seeing in i ($<\sim$0.8 arcsec). They are detected because their magnitude falls within the observable range, but the lens might be blended.

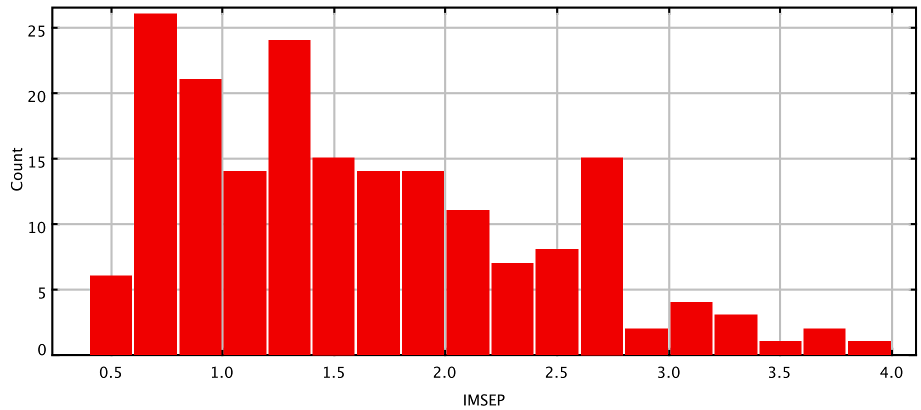

Figure 4.1: Distribution of all image separations of the i-band mock lenses in arcsec. Separation is in this case the separation between the 2 brightest QSOs.

In Figure 4.2 the distribution of apparent i-band magnitudes of the lens galaxy are shown. In red the total number of lenses, in green the double lenses and in blue the quad lenses are shown. The distribution peaks at a magnitude of 21.5. But there are also quite a few cases that are pretty bright, down to magnitude of 17. For quads and doubles the distribution seem to be relatively similar.

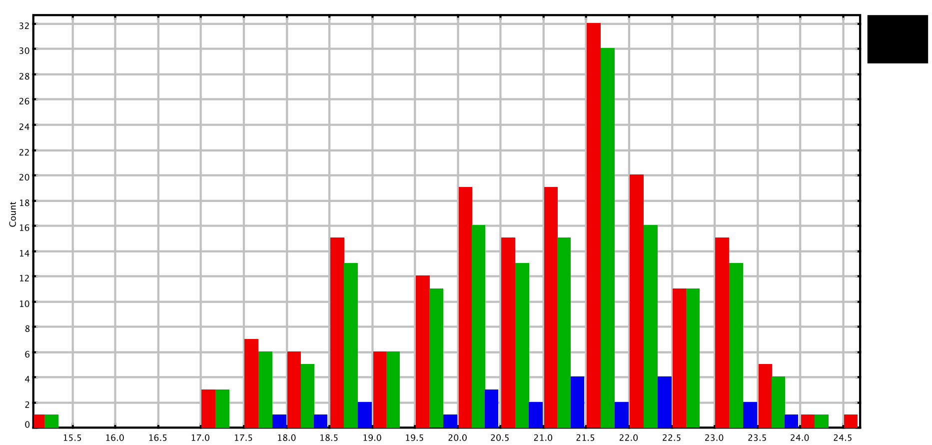

Figure 4.2: Distribution of all the magnitudes of the lensing galaxies in the mock catalog of the KiDS i-band.

In Figure 4.3 the distributions of apparent i-band magnitudes of the two QSO images of double lenses are shown. In blue the magnitude of QSO1 and in red the magnitude of QSO2. The distribution peaks at a magnitude of 21.8, but there is also quite a tail towards the brighter side, down to a magnitude of 18.8. For both images the distribution looks pretty much similar. The images seem in general to be a little bit fainter than the magnitude of lensing galaxies, but the differences are small.

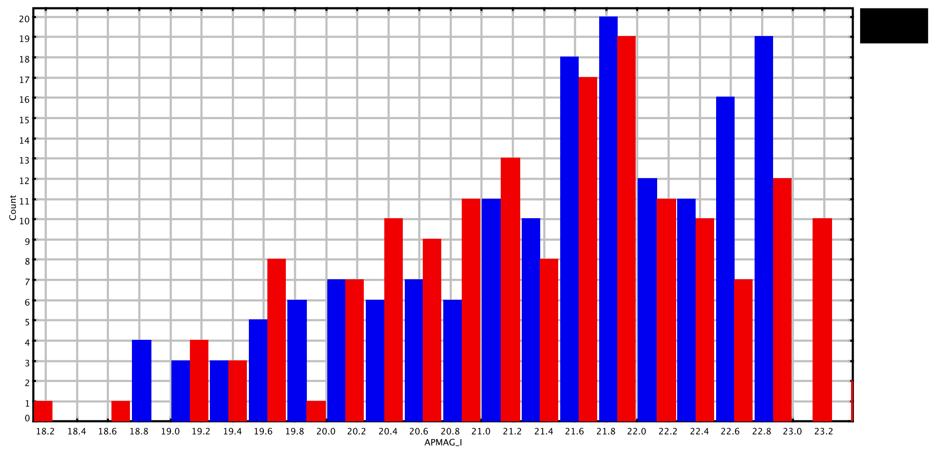

Figure 4.3: Distribution of all the magnitudes of the QSO images of double lenses in the mock catalog of the KiDS i-band.

In Figure 4.4 the distributions of apparent i-band magnitudes of the four QSO images of quad lenses are shown. In red the magnitude of QSO1, green QSO2, blue QSO3 and black QSO4 are shown. The distribution peaks at a magnitude of 22.5, but there also seems to be quite a spread towards brighter side, down to a magnitude of 20.5. For all images the distribution looks pretty much similar.

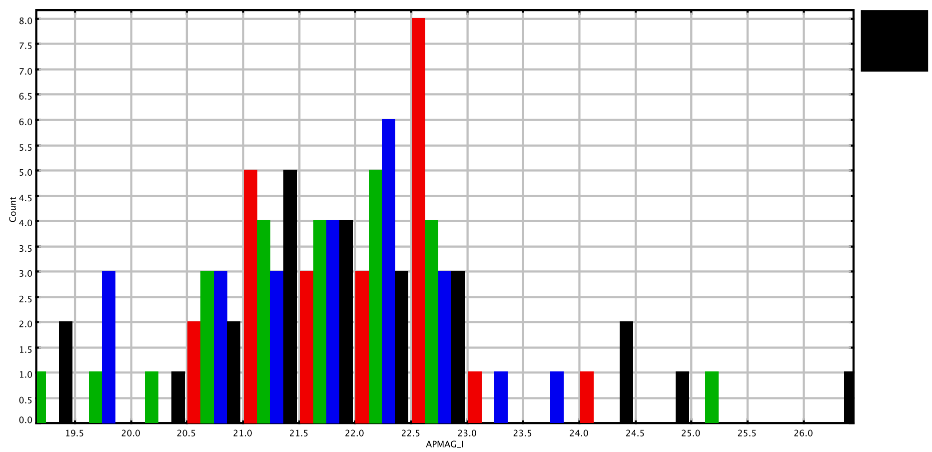

Figure 4.4: Distribution of all the magnitudes of the QSO images of quad lenses in the mock catalog of the KiDS i-band.

4.2.2 Lens-Quasar Magnitude ratio

To get a feel of what we will detect in observations, it can be useful to calculate in how many cases the lens will be brighter than the combined QSO images, and vice versa. This is especially interesting when you take an aperture that will contain all the QSO images and the lens at once. We can do this by adding up the total flux of the QSOs images and calculate their total magnitude. Then we can take the ratio of the magnitude of the lens compared and the source. It turns out that in 62% of the cases the QSO images will in total be brighter than their corresponding lensing galaxy.

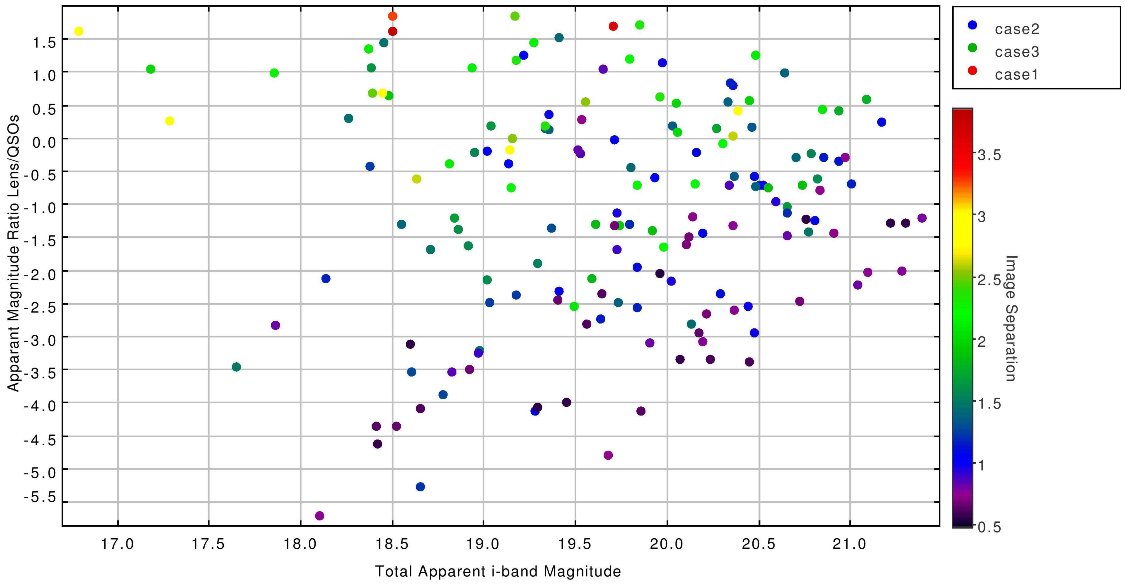

Figure 4.5: Distribution of all the magnitudes of the QSO images of quad lenses in the mock catalog of the KiDS i-band.

In Figure 4.5 we see a plot of the total apparent magnitude in the i-band of the whole system (lens+images) versus the magnitude ratio of the lens and the added QSO images expressed in magnitudes, color coded by the corresponding image separations. We see that as image separations get higher, the total apparent QSO magnitude is higher in most cases. We conclude that in general lens flux will dominate for lenses with higher separation (> 1.5 arcsec), while QSO flux dominates for small separation lenses (< 1.5 arcsec). This is useful information considering different types of lens configuration we expect, which we all want to find in the end.

4.3 Conclusions on the Mock Lenses

Results from the mock catalog show us that typical separation of strong gravitationally lensed QSOs will be between 0.5 and 4.0 arcsec, with most cases between 0 and 2.0 arcsec. About 20% of the lenses will be on or below the seeing limit of KiDS (<∼0.8 arcsec for KiDS-i). This is a significant number, and these type of configurations could cause blending of the QSO images in KiDS. Important is also that high separation lenses (> 1.5 arcsec) will have a brighter lens, while smaller separation lenses (< 1.5 arcsec) while be dominated by QSO flux. These results have consequences for the approaches that can be developed for finding lenses with different characteristics and configurations.

CHAPTER 5

Known Strongly Lensed Quasars in KiDS

5.1 Introduction

Now that we have an idea of how many lenses we can expect in KiDS and we have some general idea of how the lenses on average will look, we still don't know how the KiDS data itself looks in reality. The only way to get a feel for how real lenses look in KiDS, is to take a look at known strongly lensed QSOs in KiDS observations. We could learn something from the known lenses, and that information might help us to develop a method for finding new strong lenses. To find the known strong lenses in KiDS we make use of the masterlens database.

5.2 The Masterlens Database

The Masterlens database is a database which has the goal to have an exhaustive and up to the moment complete compilation of all discovered strong gravitational lenses, with enough detailed observed and modeled quantities, that the information can be used easily for research, education, and outreach. It has been started as part of the Orphan Lenses Project, and the database can be visited at http://www.masterlens.org. The database is not yet publicly accessible, but it's close to being opened for general access. It will not be complete: the uniform lens modeling that is planned is a substantial effort that will require more time and resources. The database is complete enough that it has already served as the basis of several research or observing proposals. All researchers are welcome to contact the administrators to gain access to the database.

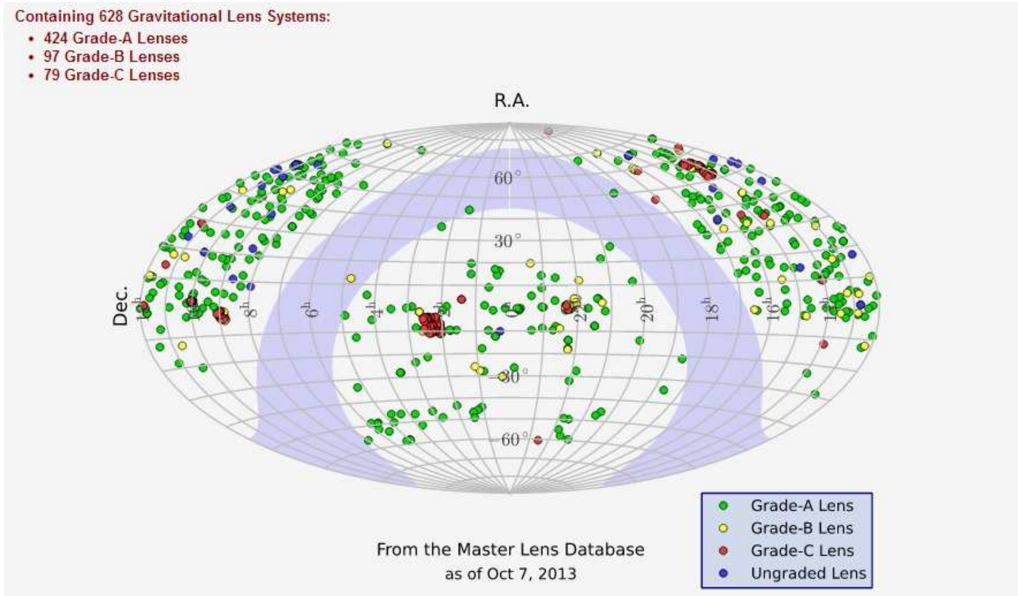

Figure 5.1: Overview of all the lenses currently in the Masterlens database. The database contains 628 Gravitational Lens Systems in total: 424 Grade-A Lenses, 97 Grade-B Lenses, 79 Grade-C Lenses.

At the moment the database consists of 628 gravitational lenses in total. Every lens is divided into a specific category. This depends on the amount of research that has been put into the specific object and the quality of available observations. A grade is given to every lens for the likelihood that the object really is a lens: grade-A = I'd bet my life, grade-B = I'd bet your life, and grade-C=I'd bet your life and you should worry. 424 grade-A lenses, 97 grade-B lenses, 79 grade-C lenses and 28 ungraded lenses.

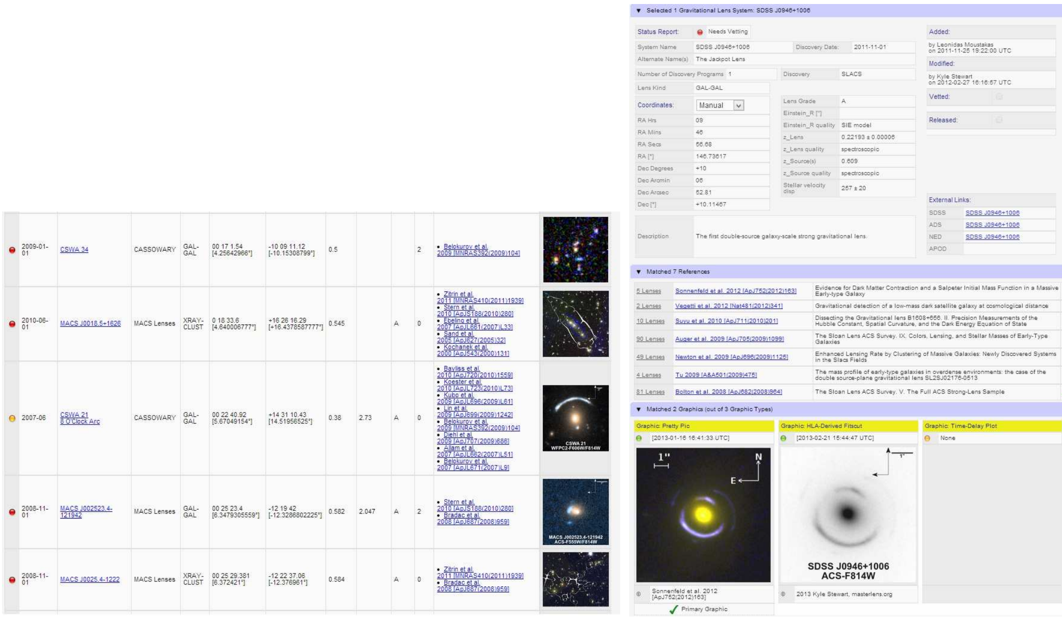

Figure 5.2: Examples of how the masterlens database looks and works.

Every lens has its own page which contains details like RA, Dec, grade, lens kind, redshift, links to publications and many more lens specific information. An example of how the database looks can be seen in Figure 5.2. The database contains 8 different lens kinds, depending on foreground-background configuration. These kinds are Galaxy-Galaxy, Galaxy-Quasars, Quasar-Galaxy, Group-Galaxy, Group-Quasar, Cluster-Galaxy, Cluster-Quasar and X-ray cluster of galaxies. For this thesis we are specifically interested in all the cases with the QSO as a background source, so Galaxy-Quasars, Group-Quasar and Cluster-Quasar specifically. The total amount of lensed QSOs is 120, of which 107 are grade-A lenses, 10 grade-B and 3 grade-C.

Table 5.1: Some important statistics from the lensed QSOs from the Masterlens database. Between brackets the number of sources the value is based on. Values of separation, z_{lens} and z_{source} are averages. Note that these values can be very biased by the choice of lenses in the survey (source:http://www.masterlens.org).

Parameter	Value
N_{lens}(QSO)	120
N_{quads}	24
$N_{doubles}$	83
Separation (two brightest QSO images)	1.423 (120) [arcsec]
z_{lens}	0.5196 (92)
z_{source}	2.105 (107)

After making a cross correlation between KiDS and masterlenses, 10 matches are found. An overview of all the matches with cutouts and data can be found at http://www.astro.rug.nl/~blokzijl/finalcutouts/masterlenses/table.html. In Figure 5.3 an overview is given of all matches between KiDS and the Masterlens database. The matches that have been observed are shown in red. There are other points inside the KiDS area, but these areas are not observed yet, so we don't have the KiDS data of those lenses.

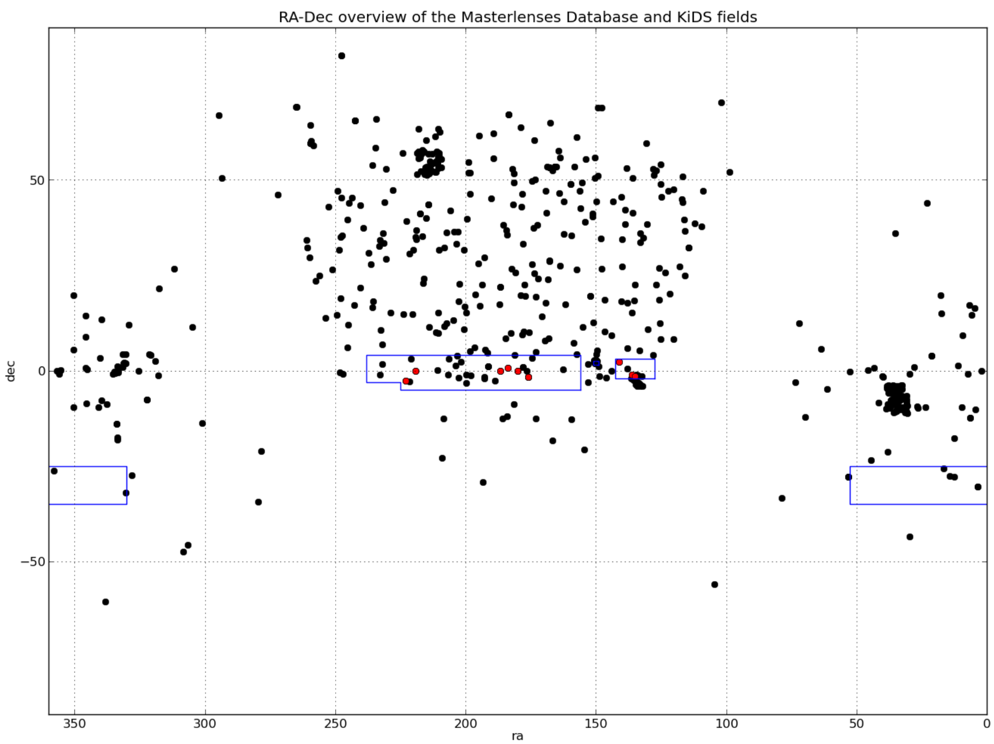

Figure 5.3: Overlap of KiDS with masterlenses. Red dots are the matches that have observational data.

5.3 Known Strongly Lensed Quasars in KiDS

2 of the 10 matches turn out to be strongly lensed QSOs, SDSSJ0924+0219 and SDSS J1226-0006. In Figure 5.4 we see a Hubble Legacy Archive (HLA) picture of both gravitational lenses. HLA is a joint project of the Space Telescope Science Institute (STScI), the Space Telescope European Coordinating Facility

(ST-ECF), and the Canadian Astronomy Data Centre (CADC) and is designed to optimize science from HST by providing online browsing capabilities and products for Hubble data and observations (http://hla.stsci.edu/). SDSS J1226-0006 (RA,Dec:186.53343659,-0.10063021) is a double lens system while SDSSJ0924+0219 (RA,Dec:141.232487,+2.323611) is a quad lens system. This is perfect because now we know for a double and a quad lens how they appear in KiDS.

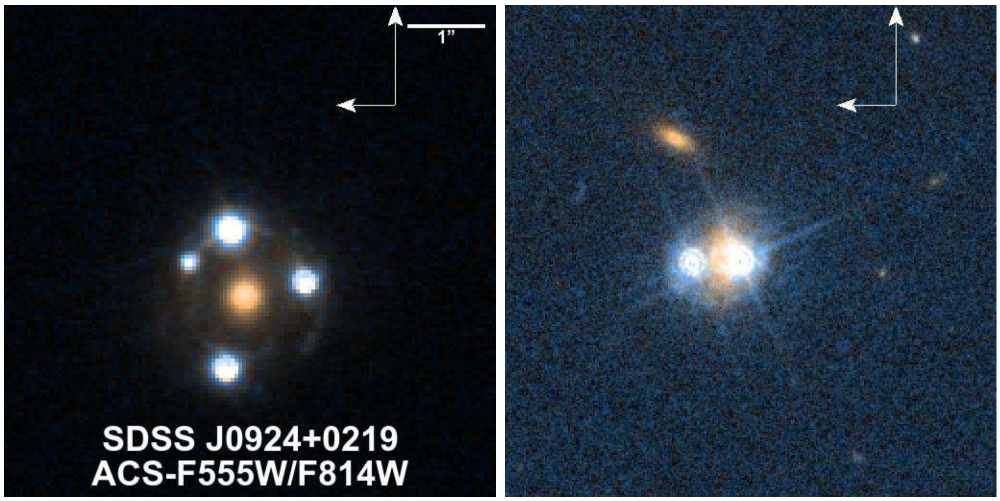

Figure 5.4: HLA images of strong gravitational lenses in KiDS. Left: SDSS J0924+0219 (RA,Dec:141.232487,+2.323611). Right: SDSS J1226-0006 (RA,Dec:186.53343659,-0.10063021)

In Table 5.2 some statistics of both lenses are shown. Both lenses are red ellipticals with redshift ∼0.4-0.5, which is in the expected range. The redshift of the QSO sources are 1.1 and 1.5 respectively, which is also in the range where we expect them to be. The magnitudes of KiDS and SDSS are shown on the right side of the table. KiDS magnitudes are taken with a 40 pixel (8 arcsec) aperture.

Table 5.2: Statistics of the known strongly lensed QSOs in KiDS. KiDS magnitudes are calculated with an aperture of 40 pixels. From left to right: right ascension, declination, redshift of the lens, redshift of the source, image separation of lens-source in arcsec, number of images,and magnitudes of KiDS and SDSS in all bands. Δ mag is the difference between the magnitude of KiDS and SDSS.

RA	Dec [deg]	z_{lens}	z_{source}	θ(separation) [arcsec]	# images		u	g	r	i deg¿deg
141.232487	+2.323611	0.394	1.524	1.87	4(quad)	KiDS	19.03	18.72	18.33	17.83
						SDSS	18.70	18.45	18.23	17.92
						Δ mag	0.33	0.27	0.10	-0.09
186.533436	-0.100630	0.516	1.123	1.24	2(double)	KiDS	19.32	18.63	18.49	17.77
						SDSS	18.84	18.63	18.08	17.93
						Δmag	0.48	0.00	0.41	-0.16

5.3.1 Strong Lens SDSS J1226-0006 in KiDS

In Figure 5.5 we see, from left to right, 15"x 15" KiDS cutouts of SDSS J1226-0006 in u,g,r and i-band, together with an KiDS-RGB image, a SDSS cutout at the same position and a HLA image of the lens. RGB images are made with the HumVI tool (https://github.com/drphilmarshall/HumVI), in which R is the KidS r-band, G = the KiDS g-band and B = is the KiDS i-band. The seeing in r is clearly the best. If we compare this to the HLA image we can see both QSO images pretty clearly. The lens elliptical is harder to distinguish, but in the RGB image we definitely see a red glow in between the two QSOs. Compared to the SDSS image, the seeing of KiDS is much better. In SDSS we see one white blob, while we can actually see the individual QSO images in KiDS quite clearly.

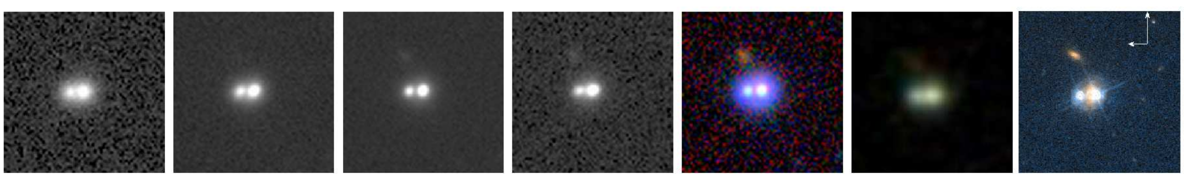

Figure 5.5: Cutouts 15" x 15" of strong gravitational lens SDSS J1226-0006 (RA,Dec:186.53343659,-0.10063021). From left to right: KiDS-u, KiDS-g, KiDS-r, KiDS-i, KiDS-RGB, SDSS and the HLA image

In Table 5.3 we give an overview of the source detections by SExtractor in all different bands. RA and Dec of every source detection are given, with their respective magnitudes, seeing, flux radius and for clarity a short description of which source it actually is in the picture. Magnitudes are again taken with a 40 pixel aperture. Important to notice is that in the r and u band, the 2 QSO images are both detected, while in the g and i band, only one source is detected at the approximate position of the lens. This might be because SExtractor detects the object as an extended source, instead of a few single point sources. The lens is not detected at all as a single source, probably because it is too faint in all observations.

Table 5.3: Source detections in KiDS on gravitational lens SDSS J1226-0006 (RA,Dec)=(186.5334366, -0.10063021). Magnitudes are calculated with an aperture of 40 pixels.

RA	Dec [degrees]	Filter	Magnitude	Mag error	FWHM(PSF) [arcsec]	Flux radius [pix]	Note degrees¿degrees
186.53350	-0.10066	u	19.319	0.051	1.054	2.81	Right QSO
186.53380	-0.10067	u	20.122	0.053	1.054	4.31	Left QSO
186.53359	-0.10064	g	18.634	0.050	0.851	4.19	In-between
186.53348	-0.10062	r	18.488	0.050	0.660	2.45	Right QSO
186.53382	-0.10064	r	19.334	0.050	0.660	2.56	Left QSO
186.53358	-0.10061	i	17.771	0.050	0.708	3.72	In-between

5.3.2 Strong Lens SDSS J0924+0219 in KiDS

In Figure 5.6 we see, from left to right, 15" x 15" the KiDS cutouts of SDSS J0924+0219 in u, g, r, and i-bands, together with an KiDS-RGB image, a SDSS cutout at the same position and a HLA image of the lens. The HLA image is not scaled and positioned to match the other images. Again, the seeing in r is the best (see Table 5.4). If we compare this to the HLA image we can see 3 of the 4 QSO images in g and r. We also see the lensing galaxy very faintly in the g and r band. If we look at the RGB image, we see 3 QSO images pretty clearly, and the lens also as a reddish blob in the middle. Again, in SDSS the seeing is worse than KiDS, and we see a big red/blue blob. We don't see or detect the 4th QSO image, which is to the left of the brightest QSO image at the top, as can be seen in the HLA picture.

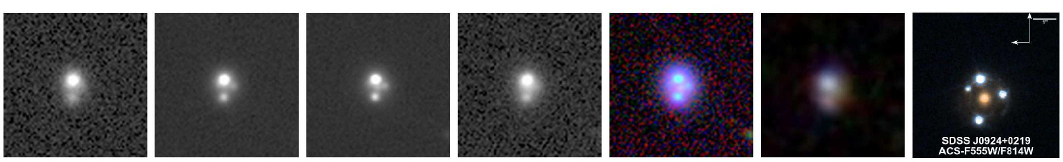

Figure 5.6: Cutouts 15" x 15" of strong gravitational lens SDSS J0924+0219 (RA,Dec:141.232487,+2.323611). From left to right: KiDS-u, KiDS-g, KiDS-r, KiDS-i, KiDS-RGB, SDSS and a HLA image. HLA image is not scaled and positioned to match the other images.

In Table 5.4 we give an overview of the source detections by SExtractor in all different bands. RA and Dec of every source detection are given, with their respective magnitudes, seeing, flux radius and a short description of which source it actually is in the picture. Magnitude are again taken with a 40 pixel aperture. Important thing to notice is that in the r and g band 2 single QSO images are detected, the bottom and the top one. The third QSO image is not detected at all, just as the lens, probably because they are too faint. In the i and u band only one source is detected. Because the seeing in i and u was higher, SExtractor probably detected an extended source instead of single points.

Table 5.4: Source detections in KiDS on gravitational lens SDSS J0924+0219 (RA,Dec:141.232487,+2.323611). Magnitudes are calculated with an aperture of 40 pixels.

RA	Dec [degrees]	Filter	Magnitude	Mag error	FWHM(PSF) [arcsec]	Flux radius [pix]	Note degrees¿degrees
141.23257	2.32360	u	19.025	0.051	1.081	4.65	Top QSO
141.23260	2.32324	g	20.271	0.051	0.794	2.78	Bottom QSO
141.23258	2.32370	g	18.722	0.050	0.794	3.25	Top QSO
141.23261	2.32325	r	19.783	0.051	0.672	2.57	Bottom QSO
141.23258	2.32371	r	18.334	0.050	0.672	3.01	Top QSO
141.23258	2.32357	i	17.827	0.050	1.036	4.94	In Between

5.4 Conclusion on the Known Lensed Quasars

From the known lenses we learned that the detection of the lensing galaxy, especially in the u and i band, is not working. When you have an RGB image you might spot it by eye, but SExtractor definitely has a hard time detecting the lens as a separate source. Therefore it is more useful to use the QSO images, which are detected much more easily by SExtractor, as a starting point for developing search methods. But the results found here can be biased by the specific types of lenses we found, which have a separation <2 arcsec, and may not be applicable to every type of strong lens there can possibly be in KiDS.

CHAPTER 6

How to Find Strongly Lensed Quasar Candidates in KiDS

6.1 Introduction

Now that we have a pretty clear picture of what we can expect of strongly lensed QSOs in KiDS, and we know that there are expected to be 20-50 unknown lenses in the completed observations right now, it's time to develop a method to start finding these lenses. In this section we explore possible ways to establish strong lens candidates for KiDS. This is especially interesting because in future surveys like LSST and Euclid the number of strong lenses to be found will be even higher (they have much more sky coverage area than KiDS) and knowing an efficient way to find the best candidates saves a lot of effort. KiDS is a perfect test case in that sense.

If you start searching for lenses in a certain survey, you want to do this as efficient as possible. Making an efficient algorithm depends on a few things. With an efficient algorithm you want to find *all* the the lenses (completeness), you want them as *fast* as possible (time), and favorably you want them at the *lowest cost* possible (cost). By exploring different methods to find strong lenses, we can argue which method is most efficient. At the end of the chapter we will do a comparison between the discussed methods, and we determine the most efficient method.

6.2 Possible Approaches

Based on the knowledge we now have about strong lenses we can think of a few different methods to start finding new ones. The most simple one is start looking by eye. We can just go through all the observations by eye and see if you can spot something interesting. Now that is gonna take a while, so there are probably better ways to make life easier. We've learned that a typical strong lens consists of a central red galaxy, with several (2 or 4) blue points sources (QSOs) close around that galaxy. So we can test the method where we use QSO or LRG catalogs from surveys that have a worse seeing than KiDS, and take a look at the KiDS data at those sources by eye to see if something interesting pops up. This is method is tested in section 6.4.1 and 6.4.2.

A different approach is to take the typical characteristics of strong gravitational lenses, which we have learned from the known and mock lenses, as a starting point. From there we can determine criteria on which we can select sources that have exactly the same characteristics as typical lensed sources. Hopefully we find strong lens candidates this way. The known lenses and mock results can be combined to find many strong lenses, but probably not all. Using this method we will try and establish our own decision tree for finding the lenses in Section 6.3.

There are some alternative approaches as well, which can be quite interesting to investigate but are not part of this thesis. These methods are discussed in Chapter 7.

6.3 Using Known/Mock Lens Characteristics

For the first method we want to test, we will start from typical characteristics of lenses learned from the known and mock strongly lensed QSOs. Because we know how a 2 real lenses look in KiDS, and we assume the mock lenses are close to reality, we can expect that other lenses also will look similar in KiDS. To decide what kind of criteria are suitable we first need to differentiate between 3 different situations that can occur when we observe a lens in KiDS (or in any survey).

6.3.1 Possible Lens Configurations in Images

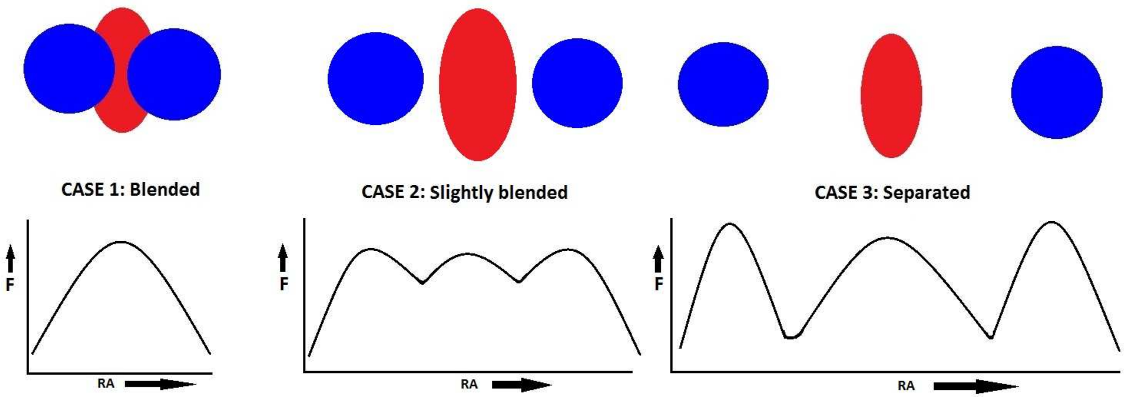

Figure 6.1: Impression of typical lens configuration expected in observations. Depending on the physical separation of the images or the seeing in a particular observation you will either end up in case 1: blended ; where the separation < seeing, case 2: slightly separated ; where the separation is on or slightly higher then the seeing, or case 3: clearly separated ; where the separation is >> seeing.

In our observations we consider 3 different types of strong lens configurations that need a different approach for finding them. In Figure 6.1 we see an impression of all three cases. In case 1 lenses the maximum separations of the QSO images is < seeing. In that case all the images blend together into one single point, and we can't distinguish single sources. If we look at the flux profile of case 1, we see that the total flux of all the sources add up to form one single point source (it might be slightly extended). In this case it will be very hard to distinguish between just a star/point source and a lens. Reasons for this situation to occur can be bad seeing or the separation of the sources is smaller than the limiting resolution of the telescope. In this situation, QSO light usually dominates over lens light, so we don't expect to detect or see a clear lens in this case.

In case 2 lenses the maximum separation of the QSO images are on or slightly higher than the seeing limit, typically 1-2 arcsec for KiDS. In this case we can distinguish a few single QSO images by eye, but the source could very well be an extended source rather than a lens. In the flux profile we see 3 peaks, but they are very hard to distinguish from each other. In this case it can happen that in the r-band, with lower seeing, you will distinguish the sources, while in for instance u-band the seeing is worse, and we can't distinguish them anymore. As we have seen with source detections by SExtractor, sometimes it will detect two sources, sometimes only one (possibly extended). It will be difficult to select against contamination of extended sources in this case.

In case 3 lenses the maximum separation of the QSO images are much larger than the seeing limit (>2 arcsec for KiDS). In this case we can distinguish all sources clearly, and probably SExtractor will detect the lens as a single sources as well. But as separations get higher, it's harder to say if the QSO images really are from the same source, and you have to select against double stars, mergers and other type of close objects.

So the task is to make a selection tree which tries to include all the three different cases described above as accurately as possible. The goal is to find as many lenses as possible, and to minimize the amount of false negatives (discard sources that are lenses in reality). The amount of contamination (false positives) is not the first concern, but it's favorably to minimize contamination because that saves time.The less sources you have to go though by eye, the less work you have to do, which saves time in the end. We don't expect to find the best decision tree right away, so we aim at making a decision tree that needs to be fine tuned as we learn and analyze what we get back. From there we can narrow down specific selection criteria until they are perfectly set. We don't want to loose any lenses by being are too hard on the selection criteria from the start on.

6.3.2 Establishing the Decision Tree

Our final decision/selection tree is shown in Figure 6.4. We will now discuss how we made this tree step by step. So we start from the sourcelist of SExtractor (step 1), which gives you a list of all detected sources in each observation, we obtain the position, magnitude and flux radius for each source. We learned from the SExtractor results (Table 5.3 and Table 5.4) on the known lenses that SExtractor does not recognize the lens as a source, because it is too faint or out-shined by the QSOs. In some cases SExtractor it did detect 2 of the QSO images, and in other cases only one. So if you find a case in which 2 QSO like source are indeed detected, it is an actual lens candidate. So to simply find 2 blue QSO-like point sources that are spatially close together is a good criteria to start with.

So the sources from the sourcelist we have need to be filtered blue point sources. Because a lensed QSO is basically a point source, the first step is to put constraints on the flux radius of all the sources in the sourcelist. From the SExtractor results we learn that the flux radius of known lenses does not go above $\sim$PSF(FHWM) (5 pix, 1 arcsec) in both u and i. So we set the flux radius to be <5 pixels.

Not all point sources of a flux radius between $0-5$ pixels will be QSOs. Many are likely to be stars or other objects that are too bright to be QSOs. Typical magnitude of lensed QSO images is around ~ 21.6 in i. Minimum magnitudes of QSO images in the mock catalog are ~ 18. To distinguish between stars and

QSOs we set our minimum magnitude cut at 17. Above a magnitude of 23, sources become very faint, and SExtractor becomes unreliable, so putting a higher limit at magnitude 23 is fine.

A typical QSO spectrum, roughly speaking, has a relatively high u band flux, and is nearly flat or gradually drops of going from u to i-band. For a typical red elliptical galaxy spectrum the exact opposite applies over the same wavelength range (see Figure 6.2 for an impression). i-band flux is higher than u band flux for most red galaxies. This fact is especially important when we consider blended lenses (case 1).

In the blended case we expect that the quasar will outshine the galaxy in u. But in the i-band a significant amount of residual flux from the lens galaxy is added, which will make the total i-band flux of the lens higher than that of a pure QSO, resulting in a lower i-band magnitude. A higher value of u-i means that the source appears more red. Therefore, the u-i value of a blended lens should be different than the u-i value of a single QSO. We expect u-i value to be slightly higher (more red) for a blended lens than for a typical single QSO, because of the residual lens flux. But we expect the u-i value of a blended lens to be lower (more blue) than the u-i value of a typical LRG. So the u-i value should be in-between the value for a typical QSO and the value for a typical LRG.

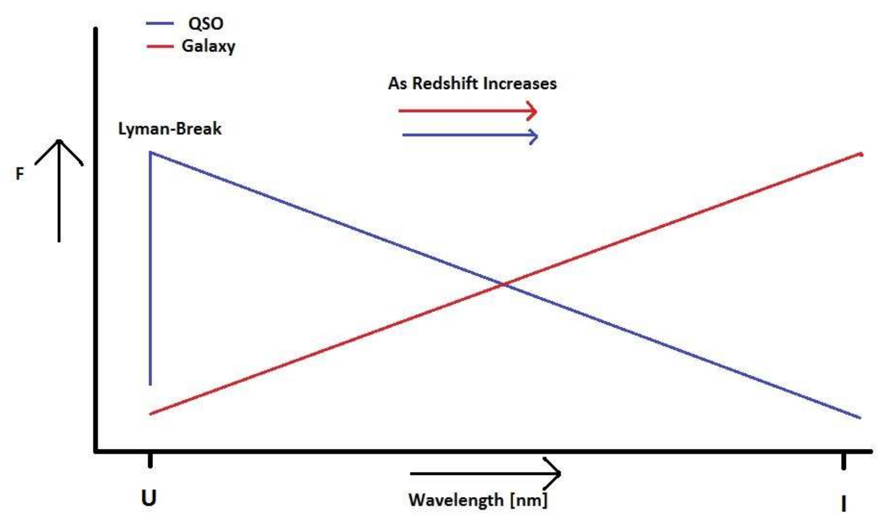

Figure 6.2: Impression of the typical shape of a QSO spectrum (blue line) and a galaxy spectrum (red line) in the visual regime.

For lenses of case 2 and 3, we should look for blue point-like sources with the u-i characteristic of a pure QSO, since the QSO image are separately detected. In Figure 6.3 a model of a QSO and LRG spectrum of u-i against redshift is shown. From this model we learn that typical u-i values for a QSO are on average around 0.4, and that value doesn't change very much over the entire redshift range. In this plot we also see that typical value of u-i for an LRG is 3.0 or higher. So above this limit we get contamination from LRGs. An upper limit of 3.0 for u-i should be fine.

In the decision tree the maximum value of u-i has been left open (letter X), which means it can be set between it can be set between 0.4 and 3.0 based on the type of lenses you want to find, or the completeness you are looking for. We will discuss completeness in the next section. Because we are using a u-i value in our method, we require that sources are detected in both u and i in step 1. Otherwise the whole method is not going to work. Sources that are not detected in both u and i are immediately discarded. Setting the flux radius, magnitude limits and maximum u-i value is step 2 of the decision tree.

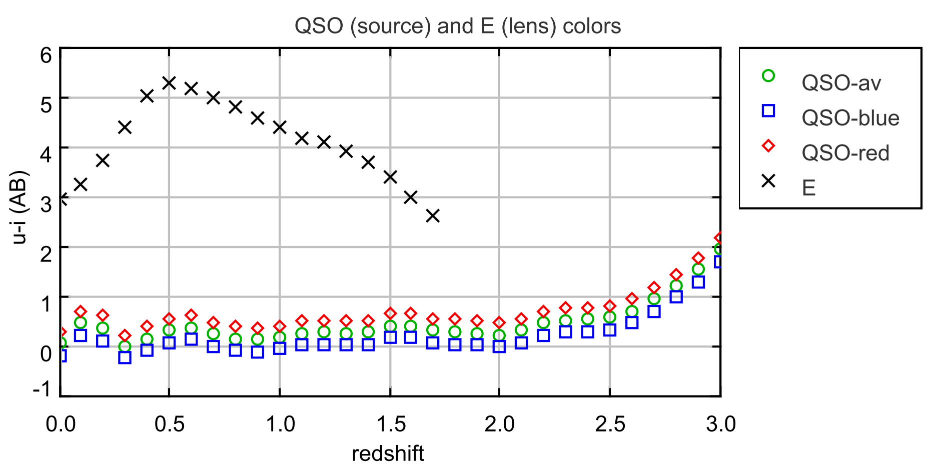

Figure 6.3: Model of typical u-i magnitudes for QSOs and Ellipticals (Kembhavi and Narlikar, 1999).

From the mock catalog and the known lenses we learned that typical separations vary between 0.5 and 4.0 arcsec, while the majority of lenses seem to have a separation between 0.5 and 2 arcsec (see section 4.2). For maximum completeness, the maximum separation is preferably set to 4, or even a little higher so you don't miss any outliers. But contamination can become higher when you include higher and higher separations, so it's a number you can play with, depending on the type of lens you want to find and the amount of contamination you accept. So we also left the value for maximum separation open in our decision tree, indicated by the letter Y in Figure 6.4 step 3. This number is preferably set between 0.5 and 4.0.

Now that we have established selection criteria for blue point like sources in u and i-band, which are comparable to the QSOs of the known lenses, we can do an internal match between all the blue point sources, to see which sources fall within the criteria you set. This is step 3. If we find a match, this is a real good candidate for being a lens (Class1). If there is not internal match, you go to step 4.

In step 4a we add the g band to the source that has not been labeled as a lens candidate in the previous step. Take the sourcelist of the g-band as a starting point. Make sure you make a cross-match the source from the previous step and the sources in the g band, in order to determine which source is the same source in the sourcelists of the u,i and g-band (step 4b). After that, make sure you put the magnitude (17-23) and flux radius constraints on all other sources of the g-band sourcelist (step 4c). From the known lenses we also learned that the maximum flux radius of the g-band should be set to 4.2 pixels. Finally, you want to do an internal separation match between your candidate and all other sources in g (step 4d). If you find a match, you have a lens candidate (Class2). If not, you continue to step 5. In step 5 you want to do the same steps as in step 4 again, but for the r band in this case. Maximum flux radius of the r band should be set to 4.2, according to the results of the known lenses. Candidates coming from this last step are Class3 candidates. All other sources will be discarded as lens candidates.

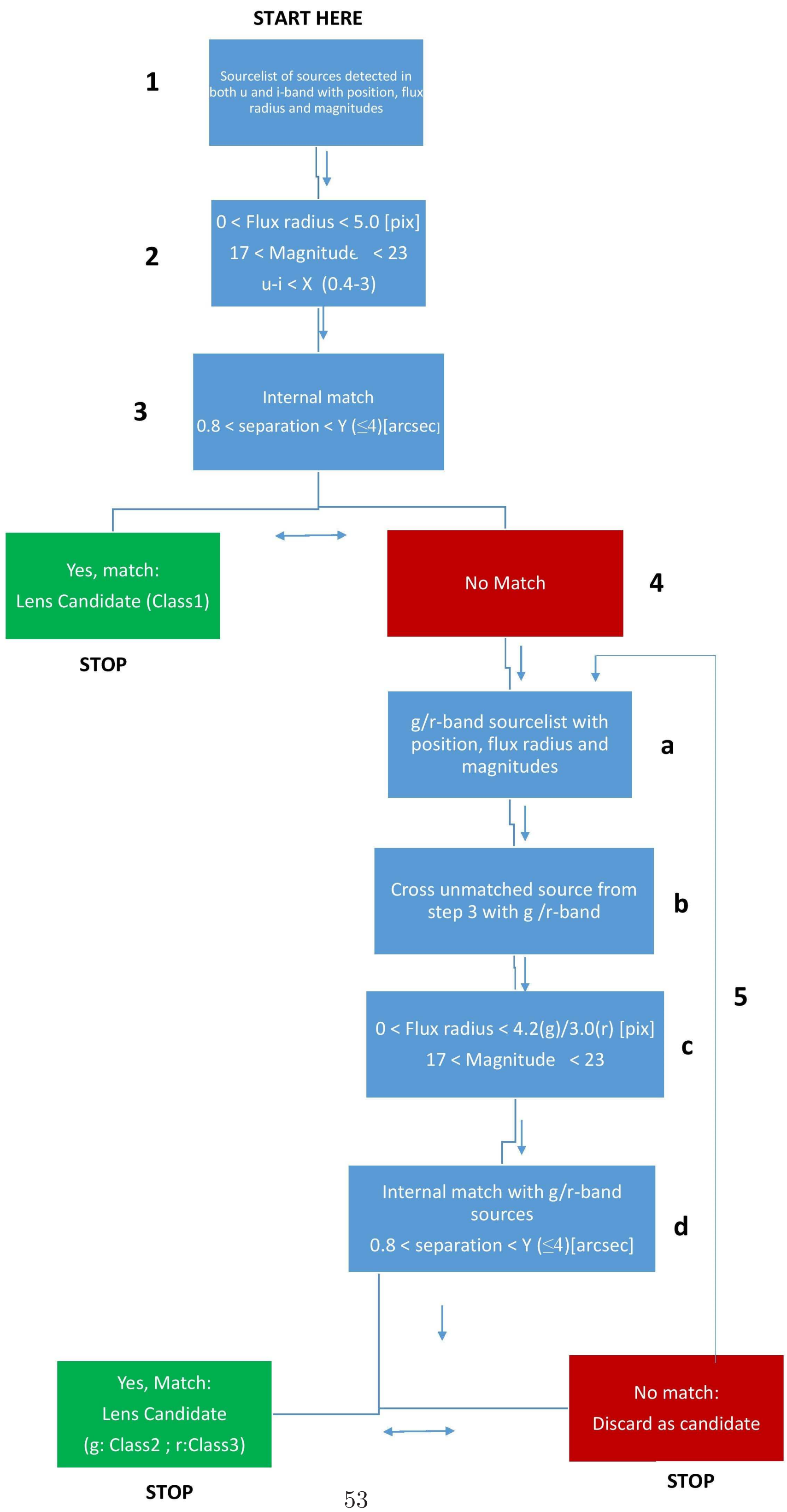

Figure 6.4: Decision tree for selecting lens candidates based on characteristics of the 2 known strongly lensed QSOs and mock characteristics.

So our final decision tree is shown in Figure 6.4. When going through the decision tree, we see that we combine the characteristics of typical strong lenses obtained from the u and i band, with the better seeing of the g and r bands. This is an optimal situation, in which you use all data of all bands to the favor of finding lenses. The final decision tree consist of 5 steps of implementation, but it is developed to be flexible, customizable and is subject to change. We will now summarize the 5 steps for clarity:

1. As a starting point, take the sourcelist of sources detected in the u and i band. Of every source you need to determine if the source exists in the u AND i band. Since we need to calculate a u-i value later on, this is an absolute requirement. Otherwise the source should be discarded.

2. On the selected sources, put the constraints described before:
   - Flux radius ≤ 5
   - $0 \leq$ Magnitude ≤ 23
   - u-i $< X$; $0.4 \leq X \leq 3.0$

3. Do an internal match between the sources of u and i. Look for pairs of sources, separated by a maximum set value: $0.8 \leq$ separation $\leq Y$; $Y \leq 5.0$ arcsec. When a source has a match, it is a very good candidate, which we label Class 1. Otherwise continue to step 4.

4. In step 4 you need to do 3 preparation steps a, b and c before you do an internal match at step 4.
   (a) Create a sourcelist of sources in the g band.
   (b) Cross match the source you have in the u/i band with the source in the g band.
   (c) Set constraints on the sources in g band
      - Flux radius ≤ 4.2
      - $0 \leq$ Magnitude ≤ 23

      Now do an internal match between the sources in g band. If we find a match, we have another candidate, which we label Class 2. If you don't find a match, continue to step 5.

5. Step 5 is exactly the same as step 4, but then for the r band. The only difference is that the max flux radius should be set to 3.0 for this step. For the r band you need to do steps a, b, c again. If we find a match, we have another candidate, which we label Class 3. If a candidate doesn't make it through this step, it can be discarded as a strong lens candidate.

6.3.3 Expected Completeness

For every type of lens it's useful to know the percentage of lenses that fall into that category. This we will call completeness. We can use completeness to compare different methods and to decide which method is best. For estimating the completeness we use the mock statistics. When we separate the mock lenses into the 3 groups as described in section 6.3 (separation case 1: <1 arcsec, case 2: 1-2 arcsec, case 3: >2 arcsec), it turns out that 29% of the lenses are of case 1, 43% are case 2 and 28% are case 3 lenses.

Table 6.1: Completeness and sub-completeness according to the KiDS i-band mock catalog of strong lenses of case 1: <1 arcsec, case 2: 1-2 arcsec, case 3: >2 arcsec for different values of u-i. Between brackets the number of lenses in the subgroup.

Case	Completeness	Sub-Completeness
u-i <3		
total	100% (188)	
case 1	29% (55)	100%
case 2	43% (80)	100%
case 3	28% (53)	100%
u-i <2		
total	88.3% (166)	
case 1	29% (55)	100%
case 2	40% (76)	95 %
case 3	19% (35)	66%
u-i <1		
total	60.6% (114)	
case 1	28% (52)	95%
case 2	29% (54)	68%
case 3	4% (8)	15%

In the decision tree we used the u-i value as a selection criteria. So we need to know this value for lenses to estimate the completeness for different values of u-i. In the mock catalog only a i-band magnitude is given, so we had to create a synthetic u-band. We made that by taking u-i = 0.4 for QSOs and u-i = 3 for the lensing galaxy. For QSOs this is fair, because the typical u-i value for QSOs is pretty constant over the redshift range, as we learned from Figure 6.3. For lenses this value is not constant over the whole redshift range, so we simplified the situation a bit here. The u and i magnitudes used for calculating the completeness in this section, are total magnitudes of the lens and QSO images together. As if you take an aperture that covers the whole lens.

For values u-i<3 the total completeness is 100%. When we set the u-i value to be <2, the total completeness changes to 88.3%. If we set u-i <1 the total completeness is 60.6%. Results, and all other completeness values per case, are summarized in Table 6.1.

Since the u-i value of the lensing galaxy isn't constant over the redshift range in reality, be we assumed it to be constant, reality might be a little bit more complicated. So the numbers/percentages might differ a little in reality, but the differentiation is assumed to be small.

6.3.4 Results

There was not time to implement and test the full decision tree, but we tried out 3 different selection methods that can be regarded as sub-trees of the full tree. These tests will give a first idea about the results of the method. These 3 methods are single blue point sources with u-i<2, blue pairs with u-i<2 and separation <10 arcsec and blue pairs with u-i<3 and separation <10 arcsec.

Single Blue Point Sources u-i<2

In the first decision tree we tried to get an estimate of how many single blue point sources we can expect per tile with u-i<2. This means both sources need to be detected in the u and i band, and need to meet the u-i requirement. The estimated completeness of this technique is 88.3%, since we expect to find all lenses with u-i<2. Results when using this technique come down to ∼1200 sources per tile which you have to weed through. These numbers are huge, so we moved on to the next method.

Blue Pairs u-i<2

In the second decision tree we narrow down the selection method to pairs of blue sources with a maximum separation of 10 arcsec, and we keep u-i<2. The estimated completeness of this technique is 59% (all separated pairs at u-i <2, case 2 + case 3). Case 1 lenses are an exception here, since we learned from the known lenses that single QSO images are not very well detected by SExtractor with this small separations, so pair detection won't work and case 1 lenses are not expected to be found with this technique. With this completeness we expect to find 3-4 lenses with this method within the 50 square degrees of DR1.

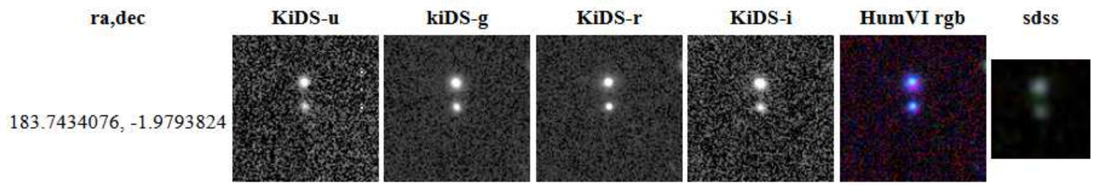

Figure 6.5: KiDS cutouts of the candidate of the selection method with blue pairs u-i<2 and separation <10 arcsec.

After running this method on DR1, we end up with 178 matches. All the cutouts can be seen at http://www.astro.rug.nl/~blokzijl/bluepairsui2/table.html. Out of these matches we find 1 good lens candidate. These candidate is shown in Figure 6.5 and the data can be found at http://www.astro.rug.nl/~blokzijl/bluepairsui2/candidates.html. Photometric properties of this source are summarized in Table 6.2.

Table 6.2: Photometric properties of the strong lens candidate with characteristic u-i<2 and separation <10 arcsec. From left to right right ascension (RA), declination (Dec), specific KiDS filter (filter), corresponding magnitude and its error, seeing and note on which source it actually is in the image.

RA	Dec	Filter	Magnitude	Mag. Error	PSF(FWHM)	Note
183.7434363	-1.978377564					
		u	21.103	0.054	0.925	Top QSO
		u	22.188	0.066	0.925	Bottom QSO
		g	19.962	0.050	0.765	Top QSO
		g	21.088	0.051	0.765	Bottom QSO
		r	19.651	0.050	0.622	Top QSO
		r	20.810	0.051	0.622	Bottom QSO
		i	19.611	0.052	1.058	Top QSO
		i	20.875	0.059	1.058	Bottom QSO

The only candidate is (RA,Dec: 183.7434363,-1.978377564). We see two blue point sources separated 1.59 arcsecs. The source is very faint, especially in u-band. But the u-i value of the bottom source is 2.37. We don't see a clear lens or a red spot in between, but the lens might be hard to see, so we can't rule out that it is a lens. At these separation we expect a lens that is about as bright as the QSO images, so it probably is not a real lens.

Blue Pairs u-i<3

The third decision tree is basically the second decision tree, but now we take u-i<3. We do this especially to see how many more contamination we can expect with this technique. Estimated completeness of this technique, according to mock, is 70.7% (all separated pairs at u-i <3 , case 2 + case 3). When we run this tree on

KiDS we find 412 matches for DR1. Results and cutouts can be seen at http://www.astro.rug.nl/~blokzijl/bluepairsui3/table.html. Out of this selection we find 3 good lens candidates, including the 1 candidates of blue pairs u-i<2. The 2 new other candidates are shown in Figure 6.6 and the data can be found at http://www.astro.rug.nl/~blokzijl/bluepairsui3/candidates.html.

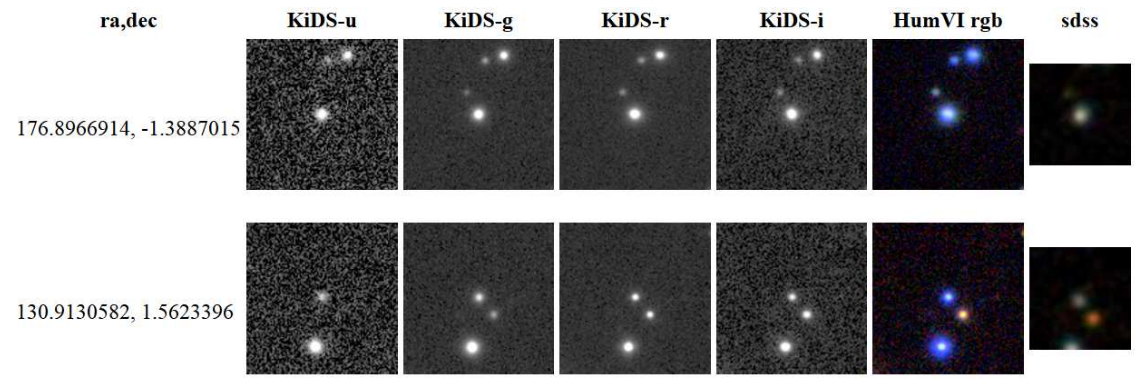

Figure 6.6: KiDS cutouts of the candidates of the selection method with blue pairs u-i<3 and separation <10 arsecs.

The first candidate is (RA,Dec:176.8966914, -1.3887015). We see actually 2 pairs of blue sources really close together. The bottom pair has a separation of 3.66 arcsec and the top pair a separation of 2.79 arcsec. We don't see something red nearby or in between a pair, which could reveal the presence of the lensing galaxy, but both pairs still are potential lenses, since the lens can be very faint. u-i vales of all blue sources are between 1.0 and 2.7, which is perfectly in the expected range for lensed QSOs.

The second candidate is (RA,Dec:130.9130582, 1.5623396). We see a very clear red galaxy, with pretty closeby, but with pretty high separation for lens, 2 blue point sources. Separation between the blue source is 7.37 arcsec. This might be a strong gravitational lens. Photometric data of both candidates is given in Table 6.3. u-i vales of the blue sources are 1.42 and 1.68, which is perfectly in the expected range for lensed QSOs. u-i color of the lens is 4.54, which is also consistent with a massive elliptical.

Table 6.3: Photometric properties of of strong lens candidates with characteristic u-i<3 and separation <10 arcsec. From left to right right ascension (RA), declination (Dec), specific KiDS filter (filter), corresponding magnitude and its error, seeing and a note on which source is actually is in the image

RA	Dec	Filter	Magnitude	Mag. Error	PSF(FWHM)	Note
176.8966914	-1.3887015					
		u	20.880	0.058	0.822	Bottom blue source
		u	24.873	0.497	0.822	Left blue source
		u	22.882	0.102	0.822	Leftmost top blue source
		u	21.393	0.063	0.822	Rightmost top blue source
		i	18.915	0.050	0.794	Bottom blue source
		i	22.101	0.069	0.794	Left blue source
		i	21.864	0.066	0.794	Leftmost top blue source
		i	19.971	0.052	0.794	Rightmost top blue source
130.9130582	1.5623396					
		u	22.118	0.071	0.966	Top blue source
		u	24.504	0.458	0.966	Lens
		u	20.363	0.052	0.966	Bottom blue source
		i	20.440	0.054	0.685	Top blue source
		i	19.964	0.052	0.685	Lens
		i	18.943	0.051	0.685	Bottom blue source

6.3.5 Additional Candidates

By accident we came across an interesting pair of blue dots, which also can be regarded as a lens candidate. The cutouts of this source are shown in Figure 6.7. Data can be found online at http://www.astro.rug.nl/~blokzijl/bluepairsui2/addcandidate.html.

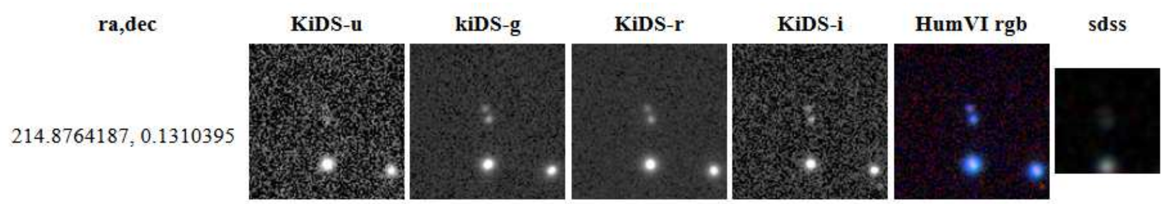

Figure 6.7: KiDS cutouts of an additional lens candidate found using selection method with blue pairs u-i<2 and separation <10 arcsecs.

The candidate is (RA, Dec: 214.8764187,0.1310395). We see 2 very nice blue dots separated by 3.66 arcseconds. In Table 6.4 the photometric data of this source is given. The magnitudes lie in the typical range for a distant blue QSO like source.

Table 6.4: Photometric properties of the accidentally found additional strong lens candidate. From left to right right ascension (RA), declination (Dec), specific KiDS filter (filter), corresponding magnitude and its error, seeing and a note on which it actually is in the image .

RA	Dec	Filter	Magnitude	Mag. Error	PSF(FWHM)	Note
214.8764187	0.1310395					
		u	23.666	0.178	1.043	Bottom blue source
		u	24.021	0.193	1.043	Top blue source
		g	22.533	0.056	0.783	Bottom blue source
		g	23.231	0.0629	0.783	Top blue source
		r	22.148	0.053	0.826	Bottom blue source
		r	22.920	0.058	0.826	Top blue source
		i	22.063	0.093	0.670	Bottom blue source
		i	22.540	0.107	0.670	Top blue source

6.3.6 Conclusion on Using Known/Mock Lens Characteristics

We developed a decision tree based on strong lens properties we learned from the known and mock lenses. The tree combines typical u-i characteristics of blue point like source, with excellent seeing in g and r, and should potentially find many lenses.

We could not test the entire decision tree, so we tested only tree sub-trees: single blue point sources with u-i<2, blue pairs with u-i<2 and separation <10 arcsec and blue pairs with u-i<3 and separation <10 arcsec. From these methods we learned that the first results look promising, though we are not convinced that the candidates we found are real lenses. The full decision tree as described, with g and r band included, has not yet been implemented and tested. This needs to be done and can hopefully yield even more interesting results in the future.

6.4 Using Existing Catalogs

6.4.1 Quasar Catalogs

The second approach we test to find new strong lenses is using existing catalogs. We know that strong lenses consist in most cases of a heavy elliptical galaxy with a few images of a QSO close by. So looking at known QSOs or LRGs might reveal new lenses. Existing catalogs may already be filtered for lenses, but higher resolution observations might reveal new interesting sources, so we give it a shot. In our case we choose the BOSS DR9 QSO catalog and the LRGS catalog as a test case.

SDDS and the BOSS DR9 QSO Catalog

In 2000, the Sloan Digital Sky Survey(SDSS) has started, and it's still ongoing. SDSS is a major, optical multi-filter imaging and spectroscopic survey using a 2.5-m wide-field optical telescope at Apache Point Observatory in New Mexico, USA. Observations are done in five color bands: u, g, r, i and z. The observations cover 14,555 square degrees on the northern sky, which is about 35% of the full sky. The galaxy sample has a median redshift of z=0.1 and goes up to z=0.7. Quasar detection reaches out to as far as z=6.

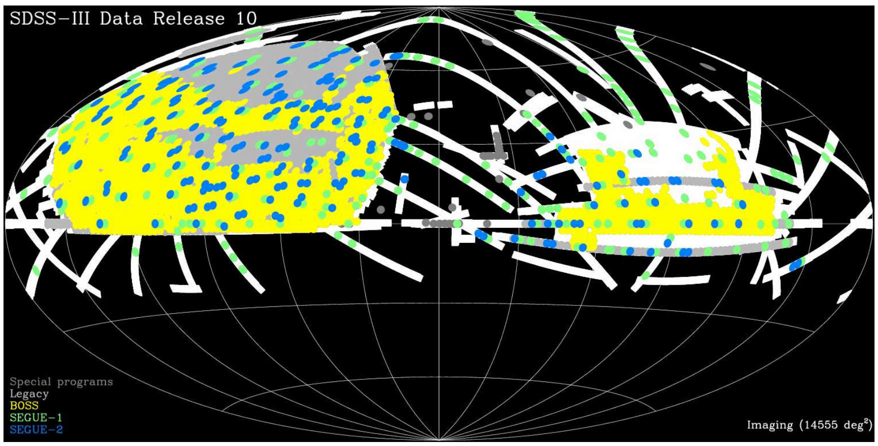

Figure 6.8: Picture of the SDSS/BOSS DR10 sky coverage.

SDSS is currently at its 10th data release (DR10), released on 31 July 2013. Besides observations in the 5 bands, SDDS DR9 also provides the first results from the Baryon Oscillation Spectroscopic Survey (BOSS) spectrograph. This means it includes about 1.5 million galaxy spectra, 230K QSO spectra and 680K star spectra.

With the release of DR9, on 31 January 2013, the BOSS spectra could be used to determine the baryonic acoustic oscillation (BAO) length scale using the Ly-α forrest. Therefore a team of researchers developed a QSO catalog containing QSOs with a redshift suitable for observing the Ly-α break in the optical range, which comes down to a redshift range of $2.2 < z < 4$. The final catalog contains about 88K QSOs. Since the BOSS QSO catalog is parts of SDSS, it also overlaps with KiDS (see Figure 6.9), so it's a suitable catalog for testing. More information can be found at http://www.sdss3.org/surveys/boss.php.

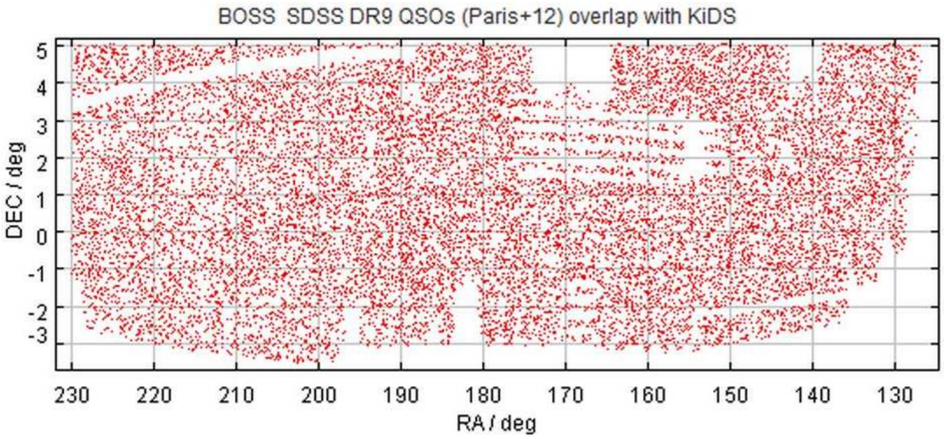

Figure 6.9: Impression of the BOSS-KiDS overlap. Red dots are the BOSS sources and the blue dots are the KiDS sources.

BOSS-KiDS Cross Correlation

After making the cross correlation between BOSS and KiDS we ended up with a list of 526 matches. The full results and an overview of cutouts can be shown at http://www.astro.rug.nl/~blokzijl/finalcutouts/BOSS/table.html and also at http://www.astro.rug.nl/~blokzijl/BOSS_KiDS_DR1DR3_only.pdf, a pdf of the html page is available (the pdf file saves loading time for the SDSS images on the web page).

BOSS Lens Candidates

After going through all the 526 matches by eye, we end up with a 2 good lens candidates. Cutouts of the 2 candidates are shown in Figure 6.10. Data can also be found at http://www.astro.rug.nl/~blokzijl/BOSS_final_selection/table.html. Photometric data of KiDS is summarized in Table 6.5. The first candidate is (RA,Dec: 180.648350676, 0.908614868996). When we compare the SDSS image to the KiDS data, we can see two blue dots, one of which is more bright than the other. In SDSS these sources are not clearly separated. The sources are 1.86 arcsec apart. We don't see anything red that might reveal the presence of a lens, but the lens might be too faint to see.

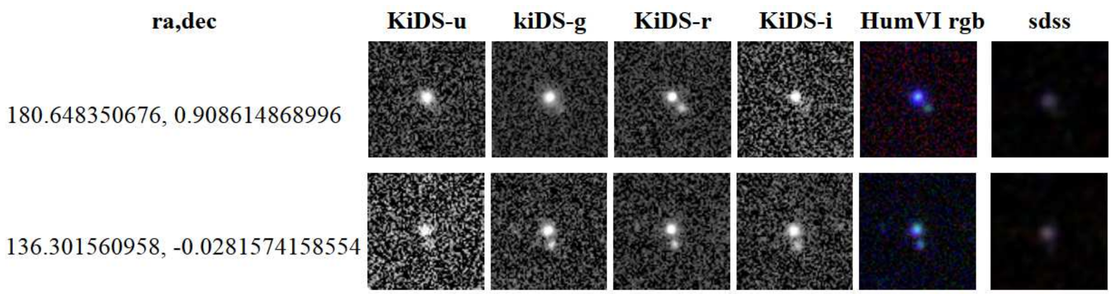

Figure 6.10: KiDS cutouts of the 2 most interesting lens candidates from the BOSS QSO catalog. Top: (RA,Dec: 180.648350676, 0.908614868996), bottom:(RA,Dec: 136.301560958, -0.0281574158554).

The second candidate is (RA,Dec: 136.301560958, -0.0281574158554). This candidate is very similar to the first candidate. We again see 2 nice blue point sources, where on the SDSS image you can't see them clearly separated. The sources are 1.79 arcsec apart. We again don't see something red, so a lens is not spotted, but it might be too faint. The separation and colors of the QSOs support the possibility that they are lenses.

Table 6.5: Photometric properties of candidates. From left to right right ascension (RA), declination (Dec), specific KiDS filter (filter), seeing, corresponding magnitude and its error.

RA	Dec	Filter	Magnitude	Mag. Error	PSF(FWHM)	Note
180.648350676	0.908614868996					
		u	21.825	0.055	1.048	Left source
		u	24.011	0.129	1.048	Right source
		g	21.299	0.056	0.915	Left source
		g	24.784	0.600	0.915	Right source
		r	21.487	0.060	0.558	Left source
		r	22.570	0.103	0.558	Right source
		i	21.344	0.065	0.791	Left source
		i	23.217	0.183	0.791	Right source
136.301560958	-0.0281574158554					
		u	22.283	0.287	0.908	Top source
		u	23.717	0.155	1.104	Bottom source
		g	21.493	0.074	0.959	Top source
		g	22.534	0.156	0.959	Bottom source
		i	21.253	0.073	0.971	Top source
		i	22.392	0.159	0.971	Bottom source

An Additional BOSS Lens Candidate

By accident we came across an interesting arc, or maybe even a ring when you look closer, at (RA,Dec: 211.6685125, -1.1365389). This is definitely a lens candidate, and might be interesting for further study. See figure 6.11 for the KiDS and SDSS cutouts of this source. Compared to the SDSS image, in SDSS we not a even see a glimpse of an arc. The cutouts can also be found online at http://www.astro.rug.nl/~blokzijl/finalcutouts/arc/table.html.

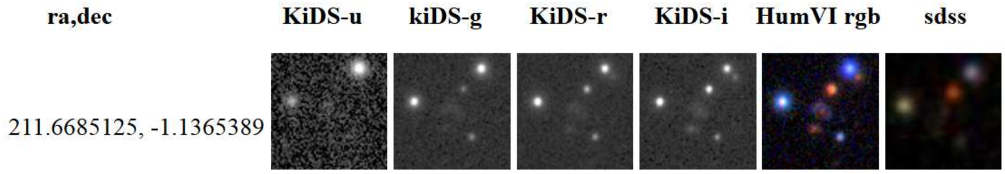

Figure 6.11: KiDS cutouts of an interesting arc found at (RA,Dec: 211.6685125, -1.1365389). This is a good lens candidate.

6.4.2 Luminous Red Galaxies Catalogs

LRGS Catalog

Another approach is to start looking at possible lensing galaxy candidates. In this case the best candidates are red elliptical galaxies, since they typically are lensing galaxies. For this we use a known luminous red galaxy (LRG) catalog, in this case the (non-official) LRGS (LRG Sample) catalog of SDSS. This catalog can be found at http://cosmo.nyu.edu/~eak306/SDSS-LRG.html.

From the mock lenses we learned that in about half of the cases the lensing galaxy is brighter than the combined QSO images for gravitational lenses. So potentially lenses could be found this way, but they will look differently than the known lenses, because they had very bright QSOs in both cases. Here we expect the LRG to be very luminous, and the QSOs might be hard to see, have a higher separations, or we might expect arcs.

Most important thing here is that the LRGS catalog also contains a number of galaxies with blueish, star-forming regions in it as well. So we have to be careful selecting lenses against galaxies with star-forming regions. This makes selecting lens candidates even harder.

LRGS-KiDS Cross Correlation

After doing the cross correlation between BOSS and KiDS we end with a list of 427 matches. The full results and overview of cutouts can be seen at http://www.astro.rug.nl/~blokzijl/finalcutouts/LRGS/table.html and at http://www.astro.rug.nl/~blokzijl/KiDS_LRGS_DR1DR3.pdf, a pdf of the html page is available (the pdf file saves loading time for the SDSS images on the web page).

LRGS Lens Candidates

Going through all the matches by eye, we end up with 2 good lens candidates: (RA, Dec: 183.889496453, -0.978593406777) and (RA,Dec:180.503235428, -0.919424621485). Cutouts of theses candidates are shown in Figure 6.12. Because we are selecting against galaxies with star-forming regions, we can not immediately determine if blue spots are indeed lensed QSOs or just parts of a galaxy. Therefore this selection is hard to make, but still very interesting. The data of both sources can be found at http://www.astro.rug.nl/~blokzijl/LRGS_candidates/table.html. Photometry of the candidates is summarized in Table 6.6.

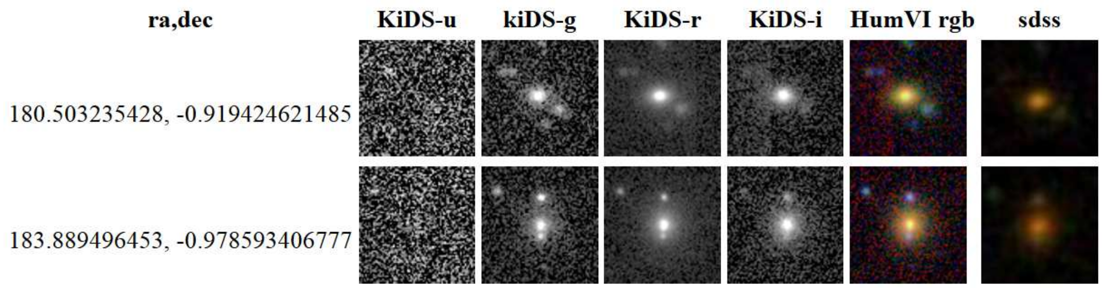

Figure 6.12: KiDS and SDSS cutouts of an the best 3 LRGS lens candidates. Top: (RA, Dec: 183.889496453, -0.978593406777) bottom (RA,Dec:180.503235428, -0.919424621485)

In the first LRGS candidate (RA,Dec:180.503235428, -0.919424621485) we see a number of blue sources/spots around the central LRG. The blue spots are at distance of 3-4.5 arcsec from the LRG, which is a pretty large separation, but still reasonable for a strongly lensed QSO. Photometry shows that values of u-i of the blue dots are between 0.3 and 2.9, which is in the expected range for QSOs. Still it's very hard to say if the blue spots are star forming regions or possible lensed QSO.

Table 6.6: Photometric properties of candidates. From left to right right ascension (RA), declination (Dec), specific KiDS filter (filter), seeing, corresponding magnitude and its error.

RA	Dec	Filter	PSF(FWHM)	Magnitude	Mag. Error	Note
180.503235428	-0.919424621485					
		u	23.496	0.309	1.126	LRG
		u	25.834	1.023	1.106	Leftmost blue source
		u	24.091	0.184	1.106	2nd leftmost blue source
		u	24.735	0.388	1.106	Bottom blue source
		u	23.456	0.258	1.106	Rightmost blue source
		g	21.263	0.059	0.809	LRG
		g	23.972	0.364	0.809	Leftmost blue source
		g	23.567	0.257	0.809	2nd leftmost blue source
		g	25.904	2.227	0.809	Bottom blue source
		g	22.760	0.134	0.809	Right blue source
		i	18.895	0.051	0.975	LRG
		i	22.923	0.138	0.948	Leftmost blue source
		i	23.441	0.192	0.948	2nd leftmost blue source
		i	24.444	0.605	0.948	Bottom blue source
		i	21.738	0.106	0.948	Rightmost blue source
183.889496453	-0.978593406777					
		u	23.704	0.805	0.983	LRG
		u	24.096	0.430	0.983	Top source
		u	30.266	85.148	0.983	Bottom source
		i	18.524	0.051	0.817	LRG
		i	20.696	0.068	0.817	Top source
		i	18.524	0.051	0.817	LRG
		i	21.991	0.097	0.817	Bottom source

In the second LRGS candidate (RA, Dec: 183.889496453, -0.978593406777) we see two blue dots that are 4.8 arcsec apart, which is quite a large separation, but not impossible.The u-i value of the top source is 3.4, while the one for the bottom source is unclear. This value is a bit high for a QSO, but not impossible. Again, the blue spots might be a star forming cloud, but a gravitational lens can not be ruled out.

Additional LRGS candidates

During the selection phase we found a few other interesting sources as well. These source are summarized at http://www.astro.rug.nl/~blokzijl/LRGS_candidates/addtable.html. We pick one out, (RA, Dec: 221.51453581, -0.671314762291), because we see a very interesting arc like feature at a distance of 2.5 arcsecs from the LRG. Cutouts are shown in Figure 6.13. This might be an arc of a gravitationally lensed source, but could also be a star-forming arm inside the galaxy disk. The other sources are not discussed here.

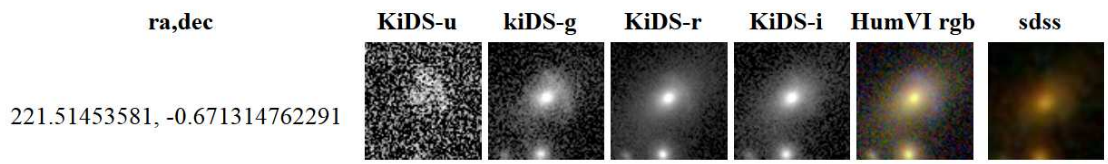

Figure 6.13: KiDS and SDSS cutouts of an additional LRGS lens candidate at RA, Dec: 221.51453581, -0.671314762291. An interesting arc is seen. It might be a lens or just a star forming region in a galaxy.

6.4.3 Conclusion on Using Catalogs

In this section we proposed to find gravitational lenses in KiDS using existing catalogs of QSOs and LRGs, and we tested this method with the BOSS and LRGS catalogs. With use of both BOSS and LRGS we found a total of 4 good candidates out of a total 900-1000 matches in 116 square degrees. We expected to find at maximum 3-4 real lenses with this technique. We only find 4 good candidates in total, none which we are convinced are a real strong gravitational lens. This number is a little bit below expectation.

Completeness of this method is low, while contamination is relatively high. Using catalogs like BOSS and LRGS seems to be not so useful, because the catalogs themselves are in most cases filtered for lenses. Because of that it is very unlikely that your really find something new. Note that our estimated completeness is optimistic, and the true completeness is probably lower because of this non-lens bias of catalogs.

6.5 Conclusion on Chapter 6

We discussed a few different approaches for finding strong lens candidates in the KiDS survey. We developed a decision tree based on typical characteristics of known and mock lenses, and tested that method partially. We also looked for strong gravitational lens candidates using existing catalogs. Both methods are not giving the results expected, and work needs to be done to refine them, but we would like to find out which method has the highest potential as it comes to finding strong lenses.

So which method of the methods we tried is in potential most efficient for finding strong gravitational lenses? Important for an efficient algorithm is the completeness and the total number of sources you have to go through (contamination). The more sources you have to go through, the more time you need to invest in finding the lenses. In Figure 6.14 we plot completeness against contamination. If you have high contamination an low completeness you end up in the left top box of the diagram (red). This is a bad situation, since you have to do much work for little results. In the case of low contamination and low completeness you have to do little work, but the results are also small (orange). This is slightly better. Favorably, you want at least a high completeness, because you want to find as many lenses as possible. That is the goal of science in the end. You can also have high contamination and high completeness, which means you have to do a lot of work, but then you have found many lenses(light green). This is pretty good. But the best situation is when you have low contamination in combination with high completeness (green!). The you have to do little work, and you find many lenses. In the end you have to make a trade-off between contamination and completeness.

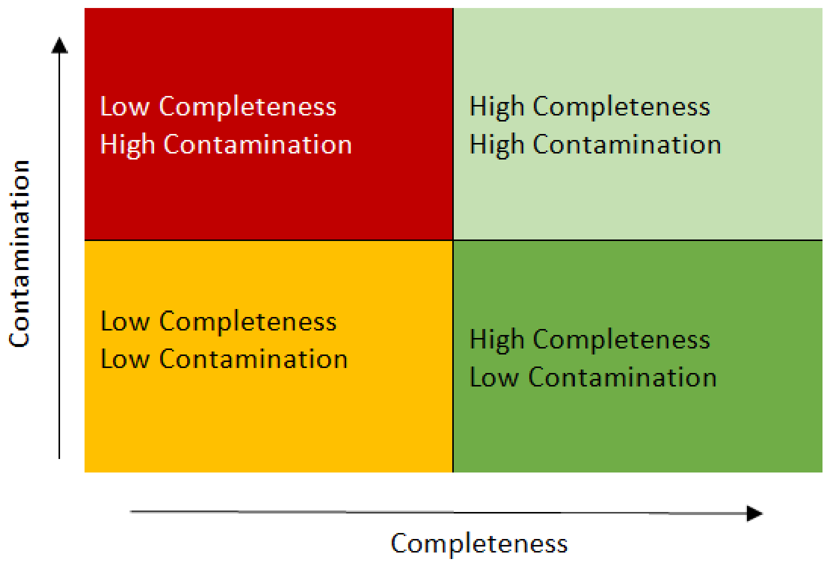

Figure 6.14: Diagram display of contamination against completeness. Favorably you want to develop a method which has high completeness and low contamination. Colors show the most favorable situation. Green for most favorably to for red most unfavorable method.

It would be great to find a method that is really fast and gives you all the lenses, and all the lenses only. Since a lot of contamination means you will need a lot of time to work through all of them, such a method is not so efficient. This will cost a lot of time and money in the end. Now let's see how our methods are placed in this spectrum.

6.5.1 Best Method

In Figure 6.15 we see an plot of all previously discussed search methods, with their corresponding value of completeness against number of sources you have to go through. The values are scaled up to the size of KiDS total, so for 1500 squares degrees instead of 50 or 116 for the different cases. This means that in case of a QSO catalog like BOSS, this value is for a hypothetical catalog like BOSS, with complete overlap with KiDS. It does not mean that it is already possible to do this in reality.

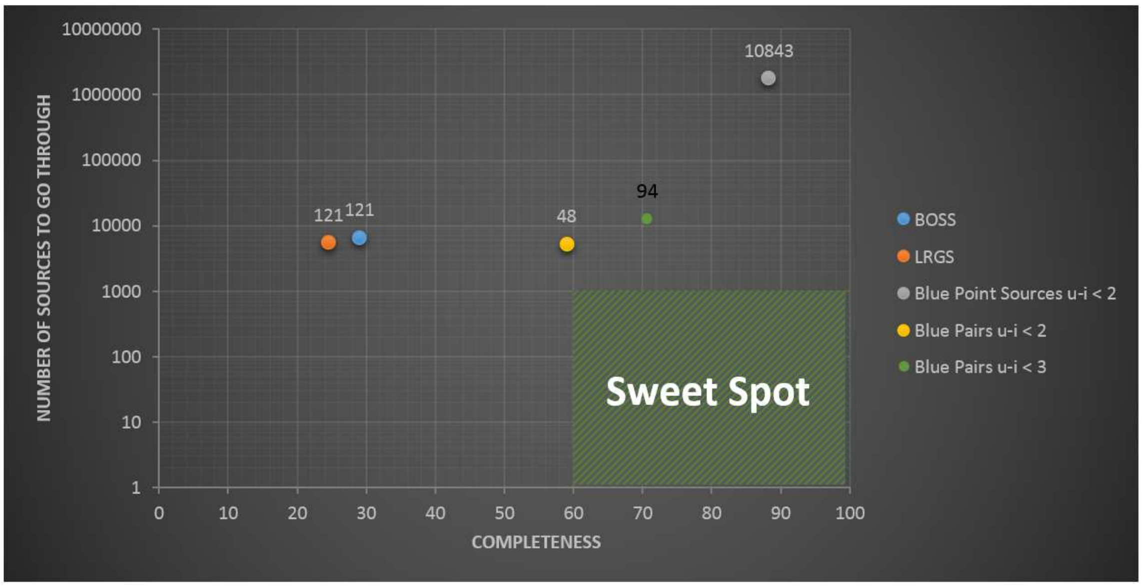

Figure 6.15: Diagram of number of sources you have to go through against completeness of the methods discussed in chapter 6. 100% completeness compares to 188 lenses. Favorably you want the method to be in the bottom-right region of the graph, to have a efficient method of finding strong lenses.

As discussed before, favorably you want to be in the bottom-right corner of the plot, where you have low number of sources to go through, and high completeness. For single blue point sources we have a staggering 1.8 million sources to go through. Compared to the other ones, this result really stands out. The values for the BOSS, LRGS and Blue Pairs u-i<2 are comparable, but the completeness of Blue Pairs u-i<2 is considerably higher. For the method Blue Pairs u-i<3, the number of lenses found is 12% higher, while the number of sources you have to go through is ~2.4 times more compared to Blue Pairs u-i<2. Therefore the method of Blue Pairs u-i<2 seems to be the most efficient technique when it comes to finding strong lenses.

The value plotted near every point in the figure is the number of sources you have to go through for every expected new found lens. This we call the contamination per lens. The value corresponding to every method means that you need to go through that number of sources (on average), to find 1 lens. For the method of Blue Pairs u-i<2 the number is 48, which is about half that of the 2nd best method Blue Pairs u-i<3, which is 94. For other methods this number is even higher. So again Blue Pairs u-i<2 does best.

In Table 6.7 an overview of all methods is given with their completeness, expected number of real lenses and the number of good candidates we expect to find in the full KiDS survey Numbers are calculated based on our results on KIDS-INT-DR3. We see that our number of good candidates is systematically lower than the expected number of lenses. This means that even if all our candidates were lenses, we still wouldn't find them all. We actually expect the number of candidates to be much higher than the number of real lenses, because we assume that a great percentage of our candidates turns out not to be a lens. A factor of 4-5 is not unreasonable. The reasons we don't find enough good candidates is not totally clear, but it might be that in the exact area of KIDS-INT-DR3, there are no real lenses that can be found this way. That would be very bad luck, but could be the case. Other reason could be that the methods simply don't work, because the r and g band are not yet included in the tests and you miss close pairs that you can only find with better seeing.

Table 6.7: Overview of all the methods of chapter 6 with their completeness, number of lenses expected and number of candidates found, scaled up to the full size of KiDS.

Method	Completeness (%)	Number of Expect Lenses	Number of Good Candidates
LRGS*	24.5	46	26
BOSS**	29	54	26
Blue Pairs u-i<2	59	111	60
Blue Pairs u-i<3	70.7	133	120
Blue Point Sources u-i<2	88.3	166	?

*Completeness of LRGS based on all sources with a brighter lens and small (<1 arcsec) and large (>2 arcsec) separation (otherwise SDSS would have found the lens): case 1 + case 3 = 24.5%.
**Completeness of BOSS based on all sources with a brighter QSO and small (<1 arcsec) and large (>2 arcsec) separation (otherwise SDSS would have found the lens): case 1 + case 3 = 33%.
NOTE: BOSS and LRGS completeness are both probably much smaller in reality because of anti-lens bias of catalogs.

But if we want to make a final comparison between the methods, we need to add the dimension of time/cost to it as well. And by the dimension of time/cost is meant, how many hours of computer+human it takes to complete a certain method, and how much that will cost in euros (roughly). To calculate this we need an overview of how many time every method takes. This overview is given in Table 6.8.

Table 6.8: Overview of all the methods of chapter 6 and the estimate time it takes to complete them. Numbers are scaled for the full KiDS survey, based on our own experience on KIDS-INT-DR3.

Method	Task	Human Time (hours)	PC Time (hours)
Using Catalogs	Making Cutouts	1	200
	Going through cutouts	35	35
	Discussing results	5	5
	Total	41	235
	Cost	€1482	
Blue Pairs u-i<2	Set and Run method in AWE	1	420
	Making Cutouts	1	60
	Going through cutouts	60	60
	Discussing results	5	5
	Total	67	545
	Cost	€2454	
Blue Pairs u-i<3	Set and Run method in AWE	1	510
	Making Cutouts	1	100
	Going through cutouts	80	80
	Discussing results	5	5
	Total	87	695
	Cost	€3184	

Cost is calculated using a value of €35 per hour for human cost, and €0.20 per hour for computer usage. Values based on 1 person working on the project.

For calculating the cost of every method we take an average salary of €35 per hour for human cost. Also computer usage costs money and although those costs are relatively minor, we still take them into account. A net price of €0.20 per hour for computer usage is fair. We calculated all numbers based on 1 person working on the method, and not more. Only discussion of results is done with someone external, but that person doesn't do the same work.

In practice we learned that using the blue pairs methods took a lot more computer time, because you need to run you selection criteria first on all data to get your candidate list. With catalogs you already have a list of coordinates which you can use immediately to start making cutouts. We can see that the Blue Pairs u-i<3 method is most expensive, while using catalogs is relatively cheap and fast.

So now we can determine which method gives you the most return on investment. When we calculate the ratio of completeness over cost we get the results show in Table 6.9. The higher the value, the more cost efficient the method it. Again Blue Pairs u-i<2 comes out as best method.

Table 6.9: Overview of all the methods of chapter 6 and their estimated completeness per euro. Numbers are scaled to the full KiDS survey. The method with the highest value is the method with the most return on investment, in this case Blue Pairs u-i<2.

Method	Completeness/Euro
Using Catalogs	0.02024
Blue Pairs u-i<2	0.02404
Blue Pairs u-i<3	0.0219

So to conclude, we compared all methods of chapter 6 by looking at their completeness, contamination and cost. When we combine all the results, it seems that the method Blue Pairs u-i<2 is most cost efficient. The method Blue Pairs u-i<3 has the highest cost, but also the highest completeness. The method Using Catalogs seems in all cases to be the most inefficient method.

CHAPTER 7

Alternative Approaches to Find Strong Lens Candidates

Now that we have tried out a few different approaches to find strong lens candidates, it's probably interesting to think about other ways to find strongly lensed QSOs. We did not look into these possibilities in this thesis, but they can be seen as a recommendation for future research on finding gravitational lenses.

- **LensTractor**: LensTractor is a piece of software made by Phil Marshall that enables you to fit nebula and gravitational lens models to your data. The software will tell you what models fits best, and that gives you knowledge whether you may have a lens of not. The software is still under development, but we spent some time working on the software already, but it isn't good enough yet for being part of this thesis. An extensive description of the software and test results can be found in Appendix A.1.
- **Stack Observations**: the first possibility is to stack the observations of all bands into one single image. Advantage of this technique would be that you combine the observations that have the best seeing with fluxes in all color bands. The resulting image could reveal something you haven't noticed before.
- **Integrate Other Available Observational Data**: what can help to get an even stronger candidate selection, is to connect your observations with observations in different wavelength ranges. For lenses this could be radio or high energy observations. For KiDS, also connecting the results with VIKING observations might be very useful.
- **Artificial Lenses**: the first thing that can be done to get even a better view of how lenses will look in KiDS, is to introduce artificial lenses in the data. In this way you can see how lenses will look in your data, because it is adjusted

to the quality of your observations. By studying artificial lenses you develop a way to start finding actual lenses.

- **Citizen Science**: to help selecting the best lens candidates out of many candidates, it might be an option to use citizen science projects like the SpaceWarps program (www.spacewarps.org). The goal of SpaceWarps is to let anyone who registers for the program, look at cutouts of images from lens candidates. The person in question then has to judge whether there is a lens in the picture somewhere, and then has to point at it with their mouse. Everyone can join SpaceWarps and start looking for lenses, and the public becomes a scientist.

  Implementation of observations into SpaceWarps requires some effort. The data has to be of reasonable quality and in a certain format before it is ready for SpaceWarps. Also, SpaceWarps makes use of artificial lenses from time to time, to test the person looking at the images. Therefore, the data needs to have some additional artificial lenses built-in. This has to be implemented. But once you have it, integrating it with SpaceWarps is a good alternative, and it can function as a second opinion.

- **Looking for arcs**: another possibility would be to use a computer bot that looks for arcs, like Arcfinder (Seidel and Bartelmann, 2007). This might not only be interesting for strongly lensed QSOs specifically, but for any type of lensing like for instance galaxy-galaxy lenses. We already found an interesting arc, discussed in section 6.4.1. This kind of software can look for all lenses that you might have missed, and could make target candidate selection complete.

These are a few ideas on how to start looking for strong lenses using a different approach than we used in this thesis. In the end, the resolution of your available data is the limiting factor for deciding whether you have a real lens or something else, so there is more work to do after you have selected candidates.

CHAPTER 8

What After You Have Established Candidates

Once you have your candidates selected, you still only have candidates. You will have to make one next step before you know if you have a real lens or not.

- **Space Telescopes**: For good lens modeling, the biggest limitation is spatial resolution for surveys like KiDS. Follow up observations with a telescope that has higher resolution is the logical next step. This can be done with a space telescope like HST, which has a superb FWHM(PSF) of 0.1. The SLACS program for instance, uses SDSS spectra to obtain lens candidates, which are observed with HST later on. Downside of this approach is that follow up with a space telescope is very expensive, and difficult to arrange.

- **Measuring Time Delays**: As discussed earlier, one can use the variability of the source QSO to measure time delays between the different QSO images. When time delays coincide, you know that 2 sources are projections of the same source, and you have a real lens. For instance, the COSMOGRAIL program uses this approach (Courbin et al., 2005).

- **radio Telescopes**: an alternative way is to do radio observations from the ground, which has very high resolution. If possible, observing variability is a very good way to confirm a gravitational lens.

These are a few main examples of what can be done after you have selected lens candidates. Keep in mind that it will be still be a time consuming and probably expensive process.

CHAPTER 9

Should We Start Looking for Strongly Lensed Quasars in KiDS: an MCA

9.1 Introduction

Now that we have picture of how many lenses we can expect in KiDS and in a number of other surveys, how much effort it takes to find them with certain methods, and in how many years we will have the results, we want to compare all those surveys against each other to see which one is most efficient. For comparing different surveys with each other we make use of what it is called a multi-criteria analysis (MCA). With the help of and MCA the survey with the highest feasibility for finding strong gravitational lenses can be determined. We will also determine how KiDS is placed in this spectrum.

9.2 Multi-Criteria Analysis

A multi-criteria analysis (MCA) is a scientific evaluation method used to chose between various alternative plans in a rational fashion using multiple different criteria. MCA originate from the field of business and policy, and are mainly used by governmental institutions as tool for decision making. An MCA is basically a cost-benefit analysis (CBA), but the difference is that the assessment criteria do not have to be expressed in monetary units. Scores can be based on economic, social or basically any other criteria you can think of that you can put a value to. The goal of an MCA is to sort the available data of a number of different plans in such a way that decision makers can use it make a decision. You can make this as complex or easy you want, but it can really help you to make complex problems transparent and more easy to understand

Considering the quest for strong gravitational lenses, we will now do an MCA. An MCA basically consists of 4 steps:

1. Problem Analysis: Decide which criteria you are going to use. Order those criteria into categories when you need to. Determine the scale you are going to use for your criteria (monetary, ratio, ordinal, nominal). Give a score for every criteria of every survey in a Table.

2. Standardization and Normalization: show all your criteria recalculated on a new scale that runs between 0 and 1, with 1 the best results and 0 the worst. In most cases this is a linear standardization function, but sometimes that can be different depending on the criteria.

3. Weighted Summation: determine what the mutual weight ratios of the criteria should be. Ask yourself: which criteria is important compared to the others? After that apply the weights to the criteria of step 2 and add up the values of the different criteria.

4. Ranking: order the result of the total weighted summation and to see which survey comes out best, and which worst

So let's apply these steps to KiDS and the other surveys discussed before, and see which survey has the best potential for finding strong lenses.

Problem Analysis

Considering the quest for strong gravitational lenses, we will now do an MCA. For scientific research into gravitational lensing there are a few criteria that are of importance. First, and probably the most important criteria is obtaining new knowledge, or scientific value. This is the goal of science in general. For the quest for strong lenses, the scientific value can in the simplest way be expressed as the total number of lenses that are possibly found in a survey. Since the expected number of lenses immediately depends on the characteristics of the survey, we don't have to consider any characteristic of the survey separately. The total number of lenses expected is our first criteria.

Another important criteria is, how fast do you have all the lenses that you expect to find. You will have all these lenses when a survey is finished. So the second criteria is the time it will take from now before you have the end results. For that we need the planned finishing year of all surveys that are discussed.

Table 9.1: Overview of some of the most important competing surveys for finding strong lenses.

Survey	N_{lens}	Years to completion (YTC)
LSST	8191	14 (2028)
PS1-3π	1963	0 (2013)
HSC-wide	614	5 (end 2015)
DES-wide	1146	3 (2017)
KiDS	450	2 (2016)

To keep it simple, we will use only these 2 criteria to determine which survey has the best relative potential of finding lenses fast and efficient. In Table 9.1 and overview of the criteria and their corresponding value is given for all the surveys we discuss.

Standardization and Normalization

In Table 9.2 the standardized and normalized values of all criteria in Table 9.1 are given. As described, all values are normalized to a scale running from 0 to 1. The most right column gives the final score of every survey in the MCA.

Table 9.2: Standardized and normalized criteria of all the surveys from Table 9.1. The most right column shows the final score of every survey in the MCA.

Survey	N_{lens}	Years to Completion	Final Score
Weight	0.6	0.4	
LSST	1.00	0.00	0.60
PS1-3π	0.24	1.00	0.54
DES-wide	0.14	0.79	0.40
KiDS	0.05	0.86	0.37
HSC-wide	0.07	0.67	0.28

Weighted Summation and ranking

In Figure 9.1 we show a pie chart of the weights given to both criteria. We give the number of lenses found in the survey a slightly higher weight (60%) than then years to completion (40%), because we think the scientific result is a little bit more important for a survey than the time it takes to really obtain them.

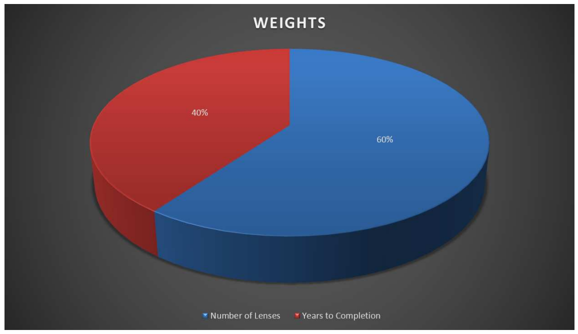

Figure 9.1: Pie chart representation of the weights added to the two criteria of the MCA. Expected number of lenses found is given a weight of 60%, while years to completion is given a weight of 40%.

When we apply these weights to the criteria shown in Table 9.2, we can determine the final ranking of surveys, which can be seen in the rightmost column. In Figure 9.2 a graphical representation of the ranking of the final MCA scores of the surveys is given. We see that the LSST survey comes out as the survey with highest ranking. The reason LSST is on top, is that it will take a while to complete from now, but the number of lenses is so huge that it still wins by the scientific achievements.

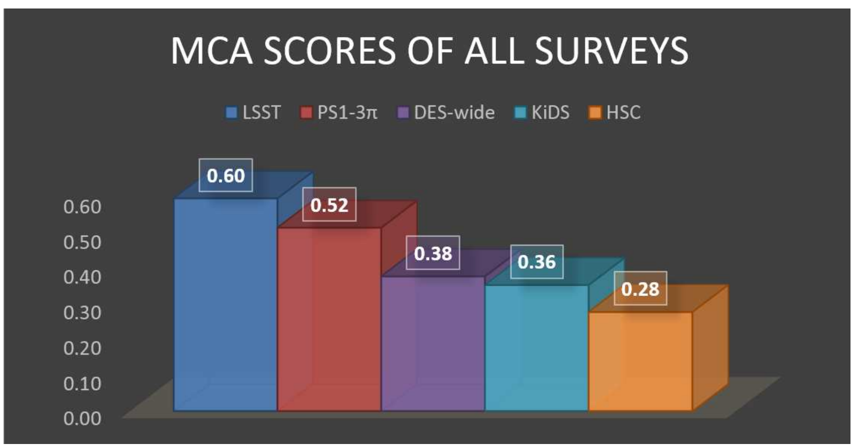

Figure 9.2: Graphical representation of the final ranking of the surveys in the MCA. LSST comes out as the best survey, while KiDS ends at place 4 out of 5.

LSST is closely followed by PANSTARRS-1/3π and DES-wide. On the 4th place finishes KiDS and last is HSC. Seeing this result, it seems that despite of the relative short time from now until KiDS has its scientific results (2 years), it still finds too little lenses compared to some other surveys, and therefore it is not the most effective survey for finding strong gravitational lenses.

CHAPTER 10

Conclusion and Discussion

The goal of this thesis was to develop and investigate ways of how to find galaxy-scale strong gravitationally lensed quasar (QSO) candidates in the Kilo Degree Survey (KiDS). To develop and investigate methods, we first needed to understand how many strong lenses we could expect and what the typical characteristics of strong gravitational lenses are. Using earlier work of Oguri and Marshall (Oguri and Marshall, 2010) we came to the conclusion that we can expect to find about 200 strong gravitational lenses in the KiDS i-band, and about 450 strong gravitational lenses in KiDS r-band. This differences arises because the PSF(FHWM) of the r-band is lower than the PSF(FHWM) of the i-band. The expected number of lenses for the r-band might not be 100% reliable because the paper is focusing on i-band only. The value of the r-band is an estimate based on the assumption that the r-band and i-band magnitudes of gravitational lenses are approximately same, because a QSO spectrum is relatively flat in the optical regime.

The second step was to investigated typical characteristics of mock strong lenses, using a piece of software developed by Oguri and Marshall called OM10. From the mock lenses we learned that about 20% of the lenses have a separation that is below the seeing limit of the KiDS i-band ($\sim$1 arcsec). Also we learned that lenses with a small separation are typically dominated by the QSO light flux, while for larger separations the lens will be brighter. This is an important difference we need to keep in mind when we want to develop a searching method.

The third step was to look at known strong lenses in KiDS. We used the masterlens database to look for known strong lenses, and we found 2 matches, a quad and a double. From those matches we learned that SExtractor is not very good at detecting the lens galaxy. Both of our lenses had good detection of the QSO images in the g or r band, but in the u and i band there were some problems, as sometimes SExtractor seemed to detect only an extended source instead of a few point sources. Using the lens as a guide for finding lenses was ruled out. Using QSO like point sources at a small separation (<4 arcsec) is possible, but KiDS r or g band seem to be more reliable when you want to use this method.

In the fourth step we investigated and developed ways to start finding new strong lenses in KiDS. We had the data of KiDS-INT-DR3 at our disposal, which is a total of 116 square degrees. We tested two methods: using existing QSO/LRG catalogs and using a self developed decision tree based on typical lens characteristics learned from known and mock lenses. We used the BOSS and LRGS catalogs to test our first method. Completeness of this method is not expected to be high (<30%), because catalogs are typically filtered for lenses. But better seeing of KiDS might yield some results, so we gave it a shot. We found 4 good lens candidates, none of which we are convinced of is a real lenses. Using the second approach, we developed a decision tree for finding strong lenses based on typical separation and u-i values of blue point sources consistent with QSOs. This tree can be used a basis, from which different sub-trees can be made and tested. We did not have the time to test the full decision tree, so we tried 3 different methods derived from it, and analyzed the results to see if we would find something promising. The 3 methods were single blue point sources with u-i <2, blue pairs with separation <10 arcsec and u-i <2, and blue pairs with separation <10 arcsec and u-i <3.

While the method of single blue point sources with u-i <2 has a very high expected completeness (88.3%), it has large amounts of contamination so it will take a lot of time to find the candidates. We did not even try to look for candidates, since that would be a big effort. The method blue pairs with separation <10 arcsec and u-i <2 gave us theoretically low contamination for relatively high completeness. With this method we found 1 good candidate, of which we are not really convinced it is a lens. The method blue pairs with separation <10 arcsec and u-i <3 gives more (a factor of 2.5) contamination than blue pairs with separation <10 arcsec and u-i <2. We found 2 good candidates, but again we are not convinced that on them is a lens.

We compared all methods against each other based on completeness, contamination and estimated cost. The method blue pairs with separation <10 arcsec and u-i <2 came out as the method with the highest potential, but the results of all methods are a little bit disappointing. It might be that we were just unlucky, just looking at a place in the sky where no lenses where detectable for KiDS. But it could very well be that our methods are not yet good enough to find them.

After that we gave an overview of other methods that might be used to start finding strong gravitational lenses, which are not tested in this thesis, but might be useful for anyone working on the subject of strong lenses. After that we gave thoughts on how to continue research after you have found interesting candidates. This can be used a reference for ideas on this subject.

In the last section we did a multi-criteria analysis (MCA) between KiDS and some other surveys with potential for finding strong gravitational lenses. It is interesting to have an idea of how feasible KiDS is for finding lenses compared to other (future) surveys. KiDS came out 4th out of 5 surveys, so it does not seem to have the potential of finding strong lenses compared to some other survey like LSST for instance.

CHAPTER 11
Future Prospects and Recommendations

So now I want to give my thoughts on what should be done after this thesis has finished. Work needs to be done to fine tune the searching methods. Using existing catalogs definitely seems not to be the way to go. We are heading in the right direction with the decision tree, especially because completeness with respect to contamination seems to be getting more and more maximized. Until now, the g and r band are not yet implemented, but the lower seeing in those bands has a great potential for getting better results. The decision tree described in section 6.3.2 is promising, and implementation of this tree is still recommended before deciding if this method is going to work at all.

One thing that is missing in the decision tree, is the detection of the lensing galaxy. It might also be interesting to investigate methods that include detecting potential lensing galaxies. This method could also yield extra lenses, which could raise completeness.

The results of the MCA show that KiDS is not the most feasible survey for finding strong lenses. It's up to the KiDS consortium to decide whether they want to continue to invest in the research for finding strong lenses.

As a final recommendation, LensTractor seems to be a promising tool for the future to help in the search for good lens candidates. We have been studying how LensTractor works, and an extensive appendix about LensTractor is added to this thesis in Appendix A.1 for further information.

Acknowledgment

I am happy to finish this thesis. Many thanks go out to Gijs Verdoes-Kleijn, Hugo Buddelmeijer and Leon Koopmans for helping me bringing this thesis to the final result and always being available for questions and further support. I would like to thank Gerjon Mensinga and Marten Hutten for mental support during the heavy and long study hours I spent on this thesis. Besides that, my thanks also go out to Phil Marshall, Joel Brownstein, Edwin Valentijn, Johnson Mwebaze, Danny Boxhoorn and Kor Begeman for helping me in all kinds of ways during the project.

I hope this work will be appreciated in the field of strong lenses, and you can always contact me for information or thoughts on anything regarding strong lenses at blokzijl@astro.rug.nl.

Cheers,

Casper Blokzijl

Appendices

APPENDIX A

LensTractor

A.1 Using Software Bots

A.1.1 LensTractor

Especially for lensed QSOs, Phil Marshall is developing a robot called LensTractor (LT). Taking as input a set of cutout images with corresponding variance map and PSF information, LT fits two models: a Nebula (consisting of an extended galaxy and N point sources), and a Lens (an SIS+shear mass distribution centered on an extended galaxy, with a point source behind it). It then does an approximate Bayesian model selection to quantify the relative appropriateness of the lens model. Nebula should always provide a better quality of fit, because it is more flexible - but sometime Lens will be an equally good fit, and because it is a simpler model, its Bayesian evidence will be higher.

Code is still under development (mainly on tweaking initialization), but it is open source and downloadable at the github: https://github.com/davidwhogg/LensTractor. Thanks to the work of Hugo Buddelmeijer, LT has already implemented compatibility for KiDS files, and it works fine on the AWE prompt. For more information on running LensTractor on AWE at the Kapteyn, or go to http://wiki.astro-wise.org/projects:kids:lensing:stronglensing:lenstractor.

A.1.2 LensTractor Input

LT uses 2 types of files as input: a coadded frame and a variance map. For the example files belonging to LT (clover leaf quad lens), the units of the files are in photons. For KiDS, this is not the case. More importantly, KiDS does not have var files at our disposal, so we have to compute them ourselves. KiDS does have weight frames belonging to every coadd. The var files of the LT examples contain sky noise and read-out noise as well as source noise, while the weight frames KiDS only have sky noise and read-out noise (Astro-WISE, 2010). For constructing the right var files for LT, we need to calculate and add the source noise to the weight frames, and than convert the units to photons. For this conversion the effective gain, G_{eff}, is used, which is known for every observation.

$$var = \sigma^2 = \frac{1}{weight} \tag{A.1}$$

We know that the variance and the weight depend on each other following equation A.1. Now we need to add the source noise to the weight files. The source noise is basically Poisson noise, which goes like:

$$\sigma(Poisson, e) = \sqrt{N(e)} \tag{A.2}$$

Where N(e) are the number of electrons. Because the coadds from the KiDS observations consist of 5 stacked observations, we need to correctly add this is up. Therefore we divide by the square root of the number of observations. We finally end up with equation A.3

$$var = \sigma^2 = \frac{1}{weight} \cdot G_{eff}^2 + \frac{N_{photons,source}}{\sqrt{N_{exposures}}} \cdot G_{eff} \tag{A.3}$$

A.1.3 LensTractor Models

LT fits two models: a Nebula model (an extended galaxy and N point sources), and a Lens model (a SIS+shear mass distribution centered on an extended galaxy, with a point source behind it). The Nebula model is divided into sub-models denoted by ”NebulaN”, which means it fits 1 extended source plus N=1,2,4 point sources. This model is very flexible, and in general it should provide a better fit than the Lens model. The Lens model consists of 1 extended source plus 1 background source. However, when the Lens model fits well, it does with fewer parameters, so it should win by Bayesian Information Criterium (BIC) value.

The software can run in 3 different modes. It can either fit the Nebula model only, fit the Lens model only, or fit both in sequence. When running in sequence, the Lens models takes results from the Nebula fit to initialize the Lens model before fitting.

A.1.4 LensTractor Output

For every model that has been fitted (nebula1, nebula2, nebula4 and lens), LT give you the values of chi-squared, number of data points N (which is basically number of pixels in the input file), number of free parameters K, the Bayesian information criterium (BIC) and the reduced chi-squares value. The BIC value is calculated using equation A.4.

$$BIC = \chi^2 + K * ln(N) \tag{A.4}$$

The value for chi-squared is calculated using equation A.5.

$$\chi^2_{red} = \frac{\chi^2}{N - K - 1} \tag{A.5}$$

Together with theses value, LT also makes plots during every step of the fitting process of all the models. These files are saved to the disk as PNGs. See Figure A.1 for an example of this output.

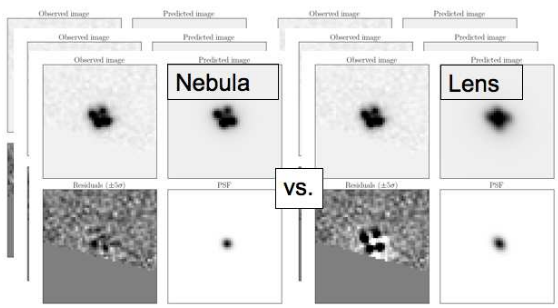

Figure A.1: Example of the output images that LensTractor generates.

As said before, the code is still under development. The nebula model should in general have a better fit compared to the lens model. We will compare relative numbers of both fits to conclude whether a nebula or lens fit is best. In general, a reduced chi squared value close to 1 is best. A value much higher than 1 means a bad fit, and a value lower than 1 means over-fitting (because of too many free parameters for instance).

A.1.5 Results on Selections

To test if LT is helpful for finding new gravitational lenses, we first want to get a picture of what values LT generates when fitting different types of sources. Therefore we test LT on some QSOs and LRGs, then on the real lenses, and finally on our candidates, to see how the values compare. We also give the output of the LT example (the cloverleaf quad lens) as a reference. The cloverleaf is not observed with KiDS, but it's a real lens, so when can use the results of LT on this example to see how our selection compares.

We took 4 QSOs, 1 LRGs, 2 real lenses, 2 BOSS lens candidates and 2 LRGS lens candidates from KiDS data. Information about all the used sources are summarized in Table A.1. An overview of the selection can also be found at http://www.astro.rug.nl/~blokzijl/finalcutouts/LT_selections/table.html

Table A.1: Overview of the selection of sources and their RA,Dec that are chose to be evaluated with LensTractor. The table consists of 1 LensTractor example (cloverleaf) 4 QSOs, 1 LRGs, 2 real lenses, 2 BOSS lens candidates and 2 LRGS lens candidates.

Type/Source info	RA	Dec
Cloverleaf	213.9416667	11.4952778
QSO-1	180.43655	-0.15138
QSO-2	185.91088	0.39621
QSO-3	176.43693	1.17333
QSO-4	133.29759	0.93532
LRG-1	178.51994	0.60517
Real Lens-1	141.23249	2.32361
Real Lens-2	186.53344	-0.10063
Lens Candidates		
BOSS-1	180.64835	0.90861
BOSS-2	136.30156	-0.02816
LRGS-1	180.50324	-0.91942
LRGS-2	183.88950	-0.97859

We want to point out that there are some inconsistencies in the output LT generates. Every time LT fits an image, it gives a different output values of chi squared. Sometimes the value of the reduced chi squared can vary quite a bit. In Fig A.2 we see the variation of reduced chi squared values over the course of 20 consequent fits of the cloverleaf example. While for nebula2 and nebula4 the fit is quite constant over the range, the value of nebula1 is quite unstable, but especially the value of the lens fit is not very constant. In one run the reduced chi squared value >10, which is even outside the plot.

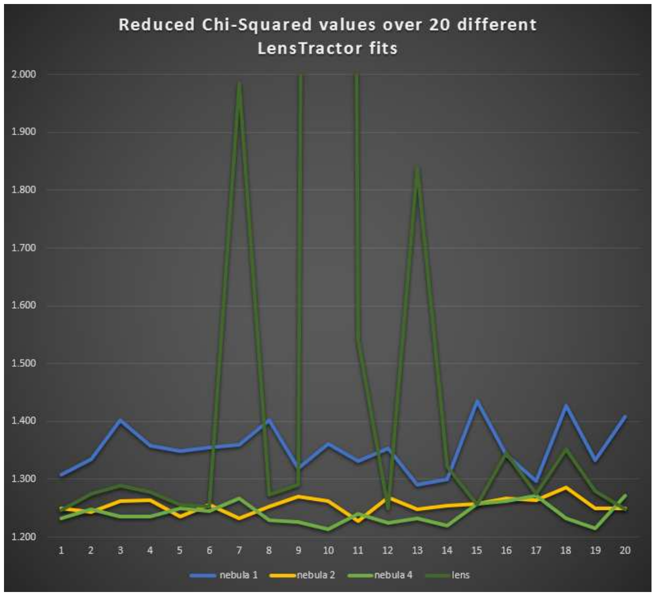

Figure A.2: Variation of LensTractor fit values on different models of the course of 20 fits. Especially the lens fit seems to be varying quite a lot.

In Fig A.2 we see that on average, if we ignore the outliers, nebula4 fits slightly better fit than the lens. So on a real lens, nebula4 fits better than lens, but almost equally good, as expected. This results suggest that we should perhaps take the minimum value for the fit result, out of a large number of fits. 5 or 10 fits is probably enough for every source to get one that fits very good. Because we only had time to evaluate one fit on all the selected sources, we could not take minimum values out of several fits, so the results may be not 100% consistent. We try to keep that in mind during analysis.

QSOs

For QSO fits we expect the nebula1 fit to be the best fit model, because it is a single point source. Results of the best fits are summarized in Table A.2. We can see that for QSO-1 (RA,Dec:180.43655391,-0.15138347) the lens fit is the best fit in the u-band, while for the other bands nebula1 fits best. The lens fit is only slightly worse in the other bands, which is remarkable.

For QSO-2 (RA,Dec:185.91088298, 0.39620986) the results are even more remarkable, since the lens model fits best for all available bands. Is this QSO maybe a lens? For QSO-3 (RA,Dec:176.43693249, 1.17332646) we see that the nebula 4 model fits best for all available bands. The lens fit seems to be quite a bit off, but it's still not the expected result. For QSO-4 (RA,Dec:133.29758652, 0.93532288) we see that the u and i band fit with nebula 1 and the g and r band fit nebula 4 best. Best lens fit in u and i hardly differ from the nebula4 fit. In g and r the differences are larger.

Table A.2: LensTractor results on a few single QSOs.

			Best Fit Model (BFM)			Best Lens Fit (BLF)		
RA	Dec	Filter	Red χ^2	Fit Type	Fit Type	Red χ^2	Fit Type	ΔBFM-BLF
180.43655391	-0.15138347	u	0.807	lens	both	0.807	both	0.000
180.43655391	-0.15138347	g	0.943	nebula1	single	0.902	single	-0.041
180.43655391	-0.15138347	r	1.009	nebula1	both	0.931	both	-0.078
180.43655391	-0.15138347	i	0.800	nebula1	single	0.800	both	-0.001
185.91088298	0.39620986	u	0.815	lens	single	0.815	single	0.000
185.91088298	0.39620986	g	0.990	lens	both	0.990	both	0.000
185.91088298	0.39620986	r	1.010	lens	single	1.010	single	0.000
185.91088298	0.39620986	i	0.000	N/A	N/A	0.000	N/A	0.000
176.43693249	1.17332646	u	0.000	N/A	N/A	0.000	N/A	0.000
176.43693249	1.17332646	g	1.842	nebula 4	single	4.956	both	3.114
176.43693249	1.17332646	r	3.903	nebula 4	single	9.256	both	5.353
176.43693249	1.17332646	i	1.757	nebula 4	both	2.871	both	1.114
133.29758652	0.93532288	u	0.849	nebula1	both	0.834	single	-0.015
133.29758652	0.93532288	g	1.408	nebula 4	single	2.076	both	0.669
133.29758652	0.93532288	r	1.716	nebula 4	single	2.543	both	0.827
133.29758652	0.93532288	i	0.995	nebula1	single	0.891	single	-0.104

LRGs

We only have the results of 1 LRG fit to evaluate. Results are summarized in Table A.3. For this LRG (RA,Dec:178.51993886, 0.60517134) we see that for u nebula1 has the best while, while the lens fit is equally good. In g and i bands we see that nebula4 fits pretty good and the lens fit is off by quite a bit. For r the nebula2 model fits best, and lens is also quite far off here.

Table A.3: LensTractor results on a few typical LRGs.

			Best Fit Model (BFM)			Best Lens Fit (BLF)		
RA	Dec	Filter	Red χ^2	Fit Type	Fit Type	Red χ^2	Fit Type	ΔBFM-BLF
178.51993886	0.60517134	u	0.939	nebula1	both	0.937	single	-0.002
178.51993886	0.60517134	g	3.024	nebula 4	both	3.539	both	0.514
178.51993886	0.60517134	r	30.641	nebula2	single	39.636	both	8.995
178.51993886	0.60517134	i	10.041	nebula 4	single	12.482	both	2.441

Real Lenses

In TableA.4 we see the result of LT fits on the known real lenses discussed earlier. For the quad lens (RA,Dec:141.23248700,2.32361100) we see that for all the band nebula4 models fits best. Only for the u band the lens fit is quite close. For the other bands the lens fit is quite a bit off. For the double lens (RA,Dec:186.53343660 -0.10063021) we see that for u nebula2 models fits best, and for the other band nebula4 models fits best. All the values of the lens fits are quite a bit off. This is obviously a remarkable results, since these are real lenses.

Table A.4: LensTractor results on the real known lensed discussed earlier.

			Best Fit Model (BFM)			Best Lens Fit (BLF)		
RA	Dec	Filter	Red χ^2	Fit Type	Fit Type	Red χ^2	Fit Type	ΔBFM-BLF
141.23248700	2.32361100	u	1.008	nebula 4	single	1.525	both	0.517
141.23248700	2.32361100	g	2.771	nebula 4	single	22.566	both	19.796
141.23248700	2.32361100	r	17.411	nebula 4	single	38.884	both	21.472
141.23248700	2.32361100	i	1.263	nebula 4	single	3.230	both	1.967
186.53343660	-0.10063021	u	0.971	nebula2	single	5.142	single	4.171
186.53343660	-0.10063021	g	2.540	nebula 4	both	13.863	both	11.323
186.53343660	-0.10063021	r	3.477	nebula 4	both	18.072	both	14.595
186.53343660	-0.10063021	i	1.428	nebula 4	single	5.754	both	4.326

BOSS Lens Candidates

In TableA.5 the results of LT on the BOSS lens candidates discussed earlier are summarized. For the first candidate, BOSS-1 (RA,Dec:180.64835068, 0.90861487), we see that the lens model fits best or u and i, while for the g band nebula1 fits best and for r band nebula4. It's interesting to see that when seeing seems to get better nebula4 seems to fit better, while for the bands with worse seeing LT fits a lens. The lens fit is not far off in g and r.

For the second candidate, BOSS-2 (RA,Dec:136.30156096, -0.02815742), we see that in the the lens model fit best in the u band. For the g band the nebula2 models fits best, while the lens fit is equally good. For the r and i band the nebula1 model fits best, while in these cases also the lens models fits equally good.

Table A.5: LensTractor results on the BOSS lens candidates discussed before.

			Best Fit Model (BFM)			Best Lens Fit (BLF)		
RA	Dec	Filter	Red χ^2	Fit Type	Fit Type	Red χ^2	Fit Type	ΔBFM-BLF
180.64835068	0.90861487	u	0.851	lens	single	0.851	single	0.000
180.64835068	0.90861487	g	0.941	nebula1	both	0.913	both	-0.028
180.64835068	0.90861487	r	0.980	nebula 4	single	1.491	single	0.511
180.64835068	0.90861487	i	0.806	lens	single	0.806	single	0.000
136.30156096	-0.02815742	u	0.799	lens	single	0.799	single	0.000
136.30156096	-0.02815742	g	0.902	nebula2	both	0.897	single	-0.005
136.30156096	-0.02815742	r	0.995	nebula1	single	1.005	single	0.010
136.30156096	-0.02815742	i	0.842	nebula1	both	0.842	single	0.000

LRGS candidates

In Table A.6 the results of LT on the LRGS lens candidates are summarized. For candidate 1, LRGS-1 (RA,Dec:180.50323543, -0.91942462), we see that for u and g nebula 2 fits best, while lens fits equally good. For g the nebula4 fits best while lens fit slightly worse here. For the i band nebula1 fits better, while lens seems to fit equally good here.

For the second candidate, LRGS-2 (RA,Dec:183.88949645, -0.97859341), we see that in the u band nebula1 fits best, with the lens fit equally good. For the other bands nebula4 fits best, while for g and i lens fit almost equally good. In r the lens fits worse.

Table A.6: LensTractor results on the LRGS lens candidates.

			Best Fit Model (BFM)			Best Lens Fit (BLF)		
RA	Dec	Filter	Red χ^2	Fit Type	Fit Type	Red χ^2	Fit Type	ΔBFM-BLF
180.50323543	-0.91942462	u	0.793	nebula2	single	0.791	single	-0.003
180.50323543	-0.91942462	g	1.000	nebula2	single	0.991	both	-0.009
180.50323543	-0.91942462	r	1.894	nebula 4	both	2.261	both	0.367
180.50323543	-0.91942462	i	0.880	nebula1	both	0.864	single	-0.016
183.88949645	-0.97859341	u	0.811	nebula1	both	0.809	both	-0.002
183.88949645	-0.97859341	g	1.266	nebula 4	both	1.449	single	0.183
183.88949645	-0.97859341	r	3.156	nebula 4	single	4.336	both	1.181
183.88949645	-0.97859341	i	1.040	nebula 4	both	1.184	single	0.143

A.1.6 Conclusion on LensTractor Results

We can see that there are quite a number of very divergent results, with some of them quite remarkable. It fits a QSO as a lens, and a real lens not or not even close to a lens. There are some inconsistencies between expectations and results. I conclude that this software is far from finished, and needs a lot of tweaking before real results can be drawn on the output it generates. The code is still under construction, but is looks promising for the future.

BIBLIOGRAPHY

Astro-WISE. How to understand weights. 2010. URL http://www.astro-wise.org/portal/howtos/man_howto_weight_scheme/man_howto_weight_scheme.pdf.

I. W. A. Browne, P. N. Wilkinson, N. J. F. Jackson, S. T. Myers, C. D. Fassnacht, L. V. E. Koopmans, D. R. Marlow, M. Norbury, D. Rusin, C. M. Sykes, A. D. Biggs, R. D. Blandford, A. G. de Bruyn, K.-H. Chae, P. Helbig, L. J. King, J. P. McKean, T. J. Pearson, P. M. Phillips, A. C. S. Readhead, E. Xanthopoulos, and T. York. The Cosmic Lens All-Sky Survey - II. Gravitational lens candidate selection and follow-up. MNRAS, 341:13–32, May 2003. doi: 10.1046/j.1365-8711.2003.06257.x.

F. Courbin, A. Eigenbrod, C. Vuissoz, G. Meylan, and P. Magain. COSMOGRAIL: the COSmological MOnitoring of GRAvItational Lenses. 225:297–303, June 2005. doi: 10.1017/S1743921305002097.

J. T. A. de Jong, G. A. Verdoes Kleijn, K. H. Kuijken, and E. A. Valentijn. The Kilo-Degree Survey. *Experimental Astronomy*, 35:25–44, January 2013. doi: 10.1007/s10686-012-9306-1.

N. Inada, M. Oguri, M.-S. Shin, I. Kayo, M. A. Strauss, T. Morokuma, C. E. Rusu, M. Fukugita, C. S. Kochanek, G. T. Richards, D. P. Schneider, D. G. York, N. A. Bahcall, J. A. Frieman, P. B. Hall, and R. L. White. The Sloan Digital Sky Survey Quasar Lens Search. V. Final Catalog from the Seventh Data Release. AJ, 143:119, May 2012. doi: 10.1088/0004-6256/143/5/119.

N. Jackson. Quasar lensing. *Bulletin of the Astronomical Society of India*, 41:19, March 2013.

J.T.A.de Jong. The kilo degree survey: Data release 1. 2013. URL https://www.eso.org/sci/observing/phase3/data_releases/kids_dr1.pdf.

Ajit K. Kembhavi and J.V. Narlikar. Quasars and active galactic nuclei: An introduction. 1999. URL http://books.google.nl/books?id=vO7KDjwzUK4C.

K. Kuijken. OmegaCAM: ESO's Newest Imager. *The Messenger*, 146:8–11, December 2011.

LSST. Lsst science book. 2009. URL http://www.lsst.org/files/docs/sciencebook/SB_Whole.pdf.

J. P. McFarland, E. M. Helmich, and E. A. Valentijn. The Astro-WISE approach to quality control for astronomical data. *Experimental Astronomy*, 35:79–102, January 2013a. doi: 10.1007/s10686-012-9296-z.

J. P. McFarland, G. Verdoes-Kleijn, G. Sikkema, E. M. Helmich, D. R. Boxhoorn, and E. A. Valentijn. The Astro-WISE optical image pipeline. Development and implementation. *Experimental Astronomy*, 35:45–78, January 2013b. doi: 10.1007/s10686-011-9266-x.

S. T. Myers, N. J. Jackson, I. W. A. Browne, A. G. de Bruyn, T. J. Pearson, A. C. S. Readhead, P. N. Wilkinson, A. D. Biggs, R. D. Blandford, C. D. Fassnacht, L. V. E. Koopmans, D. R. Marlow, J. P. McKean, M. A. Norbury, P. M. Phillips, D. Rusin, M. C. Shepherd, and C. M. Sykes. The Cosmic Lens All-Sky Survey - I. Source selection and observations. MNRAS, 341:1–12, May 2003. doi: 10.1046/j.1365-8711.2003.06256.x.

M. Oguri and P. J. Marshall. Gravitationally lensed quasars and supernovae in future wide-field optical imaging surveys. MNRAS, 405:2579–2593, July 2010. doi: 10.1111/j.1365-2966.2010.16639.x.

M. Oguri, N. Inada, B. Pindor, M. A. Strauss, G. T. Richards, J. F. Hennawi, E. L. Turner, R. H. Lupton, D. P. Schneider, M. Fukugita, and J. Brinkmann. The Sloan Digital Sky Survey Quasar Lens Search. I. Candidate Selection Algorithm. AJ, 132:999–1013, September 2006. doi: 10.1086/506019.

I. Pâris, P. Petitjean, É. Aubourg, S. Bailey, N. P. Ross, A. D. Myers, M. A. Strauss, S. F. Anderson, E. Arnau, J. Bautista, D. Bizyaev, A. S. Bolton, J. Bovy, W. N. Brandt, H. Brewington, J. R. Browstein, N. Busca, D. Capellupo, W. Carithers, R. A. C. Croft, K. Dawson, T. Delubac, G. Ebelke, D. J. Eisenstein, P. Engelke, X. Fan, N. Filiz Ak, H. Finley, A. Font-Ribera, J. Ge, R. R. Gibson, P. B. Hall, F. Hamann, J. F. Hennawi, S. Ho, D. W. Hogg, Ž. Ivezić, L. Jiang, A. E. Kimball, D. Kirkby, J. A. Kirkpatrick, K.-G. Lee, J.-M. Le Goff, B. Lundgren, C. L. MacLeod, E. Malanushenko, V. Malanushenko, C. Maraston, I. D. McGreer, R. G. McMahon, J. Miralda-Escudé, D. Muna, P. Noterdaeme, D. Oravetz, N. Palanque-Delabrouille, K. Pan, I. Perez-Fournon, M. M. Pieri, G. T. Richards, E. Rollinde, E. S. Sheldon, D. J. Schlegel, D. P. Schneider, A. Slosar, A. Shelden, Y. Shen, A. Simmons, S. Snedden, N. Suzuki, J. Tinker,

M. Viel, B. A. Weaver, D. H. Weinberg, M. White, W. M. Wood-Vasey, and C. Yèche. The Sloan Digital Sky Survey quasar catalog: ninth data release. A&A, 548:A66, December 2012. doi: 10.1051/0004-6361/201220142.

F. Patat. UBVRI night sky brightness during sunspot maximum at ESO-Paranal. A&A, 400:1183–1198, March 2003. doi: 10.1051/0004-6361:20030030.

P. Schneider, J. Ehlers, and E.E. Falco. Gravitational lenses. 1999. URL http://books.google.nl/books?id=sPAIgy9QGBsC.

G. Seidel and M. Bartelmann. Arcfinder: an algorithm for the automatic detection of gravitational arcs. A&A, 472:341–352, September 2007. doi: 10.1051/0004-6361:20066097.

E. L. Turner, J. P. Ostriker, and J. R. Gott, III. The statistics of gravitational lenses - The distributions of image angular separations and lens redshifts. ApJ, 284:1–22, September 1984. doi: 10.1086/162379.

G. A. Verdoes Kleijn, K. H. Kuijken, E. A. Valentijn, D. R. Boxhoorn, K. G. Begeman, E. R. Deul, E. M. Helmich, and R. Rengelink. Monitoring the photometric behavior of OmegaCAM with Astro-WISE. *Experimental Astronomy*, 35:103–130, January 2013. doi: 10.1007/s10686-012-9325-y.

D. Walsh, R. F. Carswell, and R. J. Weymann. 0957 + 561 A, B - Twin quasistellar objects or gravitational lens. Nature, 279:381–384, May 1979. doi: 10.1038/279381a0.